Molecular Plant
Research Article

CellPress
Partner Journal

The vernalization-induced long non-coding RNA *VAS* functions with the transcription factor TaRF2b to promote *TaVRN1* expression for flowering in hexaploid wheat

Shujuan Xu[1,2], Qi Dong[1,2], Min Deng[2,5], Dexing Lin[2,6], Jun Xiao[5,8], Peilei Cheng[7], Lijing Xing[1], Yuda Niu[1], Caixia Gao[6], Wenhao Zhang[2,4], Yunyuan Xu[1,3] and Kang Chong[1,2,3,*]

[1]Key Laboratory of Plant Molecular Physiology, Institute of Botany, Chinese Academy of Sciences, Beijing 100093, China

[2]University of Chinese Academy of Sciences, Beijing 100049, China

[3]Innovation Academy for Seed Design, Chinese Academy of Sciences, Beijing 100093, China

[4]State Key Laboratory of Vegetation and Environmental Change, Institute of Botany, Chinese Academy of Sciences, Beijing 100093, China

[5]State Key Laboratory of Plant Cell and Chromosome Engineering, Institute of Genetics and Developmental Biology, Innovation Academy for Seed Design, Chinese Academy of Sciences, Beijing 100101, China

[6]State Key Laboratory of Plant Cell and Chromosome Engineering, Center for Genome Editing, Institute of Genetics and Developmental Biology, Innovation Academy for Seed Design, Chinese Academy of Sciences, Beijing 100101, China

[7]College of Horticulture, Nanjing Agricultural University, Key Laboratory of Landscaping, Ministry of Agriculture, Nanjing 210095, China

[8]CAS-JIC Centre of Excellence for Plant and Microbial Science, Institute of Genetics and Developmental Biology, Chinese Academy of Sciences, Beijing 100101, China

***Correspondence: Kang Chong (chongk@ibcas.ac.cn)**

https://doi.org/10.1016/j.molp.2021.05.026

ABSTRACT

Vernalization is a physiological process in which prolonged cold exposure establishes flowering competence in winter plants. In hexaploid wheat, *TaVRN1* is a cold-induced key regulator that accelerates floral transition. However, the molecular mechanism underlying the gradual activation of *TaVRN1* during the vernalization process remains unknown. In this study, we identified the novel transcript *VAS* (*TaVRN1* alternative splicing) as a non-coding RNA derived from the sense strand of the *TaVRN1* gene only in winter wheat, which regulates *TaVRN1* transcription for flowering. *VAS* was induced during the early period of vernalization, and its overexpression promoted *TaVRN1* expression to accelerate flowering in winter wheat. *VAS* physically associates with TaRF2b and facilitates docking of the TaRF2b-TaRF2a complex at the *TaVRN1* promoter during the middle period of vernalization. TaRF2b recognizes the Sp1 motif within the *TaVRN1* proximal promoter region, which is gradually exposed along with the disruption of a loop structure at the *TaVRN1* locus during vernalization, to activate the transcription of *TaVRN1*. The *tarf2b* mutants exhibited delayed flowering, whereas transgenic wheat lines overexpressing *TaRF2b* showed earlier flowering. Taken together, our data reveal a distinct regulatory mechanism by which a long non-coding RNA facilitates the transcription factor targeting to regulate wheat flowering, providing novel insights into the vernalization process and a potential target for wheat genetic improvement.

Key words: winter wheat, vernalization, flowering, long non-coding RNA, chromosome loop

Xu S., Dong Q., Deng M., Lin D., Xiao J., Cheng P., Xing L., Niu Y., Gao C., Zhang W., Xu Y., and Chong K. (2021). The vernalization-induced long non-coding RNA *VAS* functions with the transcription factor TaRF2b to promote *TaVRN1* expression for flowering in hexaploid wheat. Mol. Plant. **14**, 1525–1538.

INTRODUCTION

Temperature is one of the major climate factors that govern crop geographic regions and planting times (Jung and Muller, 2009). The ability of plants to sense and respond to changes in the environmental temperature is crucial to their survival and reproductive success (Zhang et al., 2019; Song et al., 2021). Low temperature can be detrimental or advantageous to the

Published by the Molecular Plant Shanghai Editorial Office in association with Cell Press, an imprint of Elsevier Inc., on behalf of CSPB and CEMPS, CAS.

growth, development, and geographic distribution of crops (Zhu, 2016; Chen et al., 2021). For example, low temperature in the seedling or reproductive stage leads to cold stress, thereby affecting the normal growth and grain yield of tropical plants such as rice (Shi et al., 2015; Guo et al., 2018). Although prolonged low-temperature exposure is required to promote flowering and improve grain yield of temperate crops such as wheat and barley (Xu and Chong, 2018; Zhang et al., 2019; Luo and He, 2020), this prolonged cold exposure is accompanied by the initiation of floral activators or the suppression of growth habits based on the vernalization requirement (Ozturk et al., 2006; Thorup-Kristensen et al., 2009). Cultivar breeders aim to use species with winter and spring habits to expand cultivation into wider regions to maximize grain yield. Therefore, it is important to understand how the winter habit is controlled.

The genetic and epigenetic regulatory mechanisms of vernalization have been well studied in *Arabidopsis* (Greenup et al., 2009; Antoniou-Kourounioti et al., 2018; Hepworth et al., 2018; Luo and He, 2020). However, cereal crops such as wheat and barley operate a different genetic network of key genes during the vernalization process (Xu and Chong, 2018). In hexaploid wheat, various regulatory genes are expressed in response to vernalization to adjust floral initiation; these include *TaVRN1*, *TaVRN2*, *TaFT1* (FLOWERING LOCUS T1)/*TaVRN3*, *TaVRN-D4*, and *VER2* (Xu and Chong, 2018; Zhang et al., 2019). During the vegetative stage of winter wheat, *TaVRN1*, which encodes an APETALA1 (AP1)-like MADS box transcription factor, is expressed at a low level (Yan et al., 2004a; Trevaskis, 2010). The floral repressor *VRN2*, which encodes a zinc-finger protein, has high expression and represses the expression of *FT1* (Yan et al., 2004b; Dubcovsky et al., 2006). *FT1* encodes a polyethanolamine binding protein and integrates photoperiod and vernalization signaling to accelerate flowering (Dubcovsky et al., 2006; Trevaskis et al., 2007). The jacalin-like lectin VER2, induced transcriptionally by vernalization, can interact with the glycine-rich RNA binding protein TaGRP2 and switch its subcellular localization from the nucleus to the cytoplasm, thereby repressing its specific RNA binding to *TaVRN1* pre-mRNA and resulting in high levels of *TaVRN1* transcripts after prolonged cold exposure (Yong et al., 2003; Xing et al., 2009; Xiao et al., 2014; Xu et al., 2019). A recent study showed that TaVRT2 (an SVP-like MADS box protein) can interact with VRN1 to form a heterodimer and promote the further expression of *VRN1* by binding to the *VRN1* promoter (Xie et al., 2019). *VRN1* transcription is initiated and increased to a high level after cold exposure in winter. High *VRN1* expression after winter cold exposure represses the transcription of *VRN2* by directly binding to its promoter, enabling the transcription of *FT1*/*VRN3* under long day conditions in the spring (Dubcovsky, 2005).

VRN1, a floral activator, is a central gene in the regulation of vernalization in cereal crops (Trevaskis, 2010). Hexaploid wheat genomes contain three copies of the *TaVRN1* gene, designated *TaVRN-A1*, *TaVRN-B1*, and *TaVRN-D1* (Loukoianov et al., 2005). *TaVRN1* is induced by prolonged cold exposure and maintains high levels of expression after vernalization (Oliver et al., 2009). Both the intact promoter and the critical region in intron1 of wheat *TaVRN1* are essential for the vernalization requirement (Fu et al., 2005). Either insertion or deletion of the promoter, or large deletions in intron1, have caused "unlicensed" expression of *TaVRN1* without cold exposure, causing wheat to switch to a spring growth habit, hinting that these regions are crucial for keeping *TaVRN1* silent before vernalization (Fu et al., 2005). One dominant *TaVRN1* allele in any of the three copies of the *TaVRN1* gene or the translocation of *TaVRN-A1* to chromosome 5DS (*TaVRN-D4*) is sufficient to confer a spring growth habit (Kippes et al., 2014, 2015). These mutations are likely to break higher chromatin organizational structures or modulate the epigenetic regulation of the *TaVRN1* locus. However, details of the molecular mechanism remain unknown, in particular at the post-transcriptional level.

Long non-coding RNA (lncRNA) (>200 nt) includes long intronic ncRNAs (incRNAs) and long intergenic ncRNAs (lincRNAs) (Mercer et al., 2009; Chekanova, 2015). Although many lncRNAs have been identified, few have been clearly studied in part because of their low expression and poor sequence conservation. In *Arabidopsis thaliana*, three lncRNAs have been shown to participate in the regulation of *FLOWERING LOCUS C* (*FLC*) silencing and the maintenance of its repressed state during or after vernalization (Heo and Sung, 2011; Sun et al., 2013; Kim and Sung, 2017; Tian et al., 2019). *FLC* encodes a MADS box transcription factor and is expressed at high levels as a repressor of flowering in the seedling stage (Michaels and Amasino, 1999). During prolonged cold exposure, trimethylation of lysine 27 on histone H3 (H3K27me3) accumulates at the nucleation zone of the *FLC* locus to initiate silencing of the *FLC* gene, which is regulated by Polycomb Repressive Complex 2 (PRC2) (Bastow et al., 2004; Questa et al., 2016; Yuan et al., 2016; Tian et al., 2019). Cold-assisted INTRONIC NONCODING RNA (COLDAIR) is the representative long-stranded non-coding RNA in plants. COLDAIR is induced by low temperature and can interact with CURLY LEAF (CLF) protein, a key component of the PRC2 complex, to recruit the PRC2 complex to the *FLC* locus for H3K27me3 modification (Heo and Sung, 2011; Kim et al., 2017; Kim and Sung, 2017). Another lncRNA, COLD-INDUCED LONG ANTISENSE INTRAGENIC RNA (COOLAIR), is upregulated in early vernalization and accelerates the transcriptional repression of *FLC* by reducing H3K36me3 in *A. thaliana* (Sun et al., 2013; Csorba et al., 2014; Marquardt et al., 2014; Ietswaart et al., 2017). An additional lncRNA, COLDWRAP (cold of winter-induced non-coding RNA from the promoter), was shown to repress *FLC* expression by retaining the PRC2 complex at the *FLC* locus in association with COLDAIR (Kim and Sung, 2017). Unlike *Arabidopsis*, cereal crops have a completely different genetic network for vernalization control. A series of key vernalization genes and their network have been reported in wheat and barley. However, the role of lncRNA in vernalization of temperate cereal plants is less well known.

Here, we identify *VAS*, a novel lncRNA that is transcribed from the *TaVRN1* locus during early vernalization treatment, specifically in wheat with a winter habit. *VAS* can facilitate the full activation of *TaVRN1* during vernalization. At the molecular level, *VAS* is recognized by RF2b and helps RF2b to bind and activate *TaVRN1*, together with RF2a, to accelerate flowering. Our data suggest that *VAS* plays an important role in the control of vernalization for winter wheat flowering.

RESULTS

VAS, an alternative splicing transcript of *TaVRN1*, is induced specifically in winter wheat

The specific site RIP-3 of *TaVRN1* is bound by GRP2 to regulate its pre-mRNA processing during wheat vernalization (Xiao et al., 2014). Unexpectedly, a splicing transcriptome screening assay showed that the novel transcript *VAS* (*VRN1* alternative splicing) from pre-mRNA of *VRN1* appeared during vernalization. Semi-quantitative RT–PCR experiments were performed to detect the response of *VAS* to vernalization in different spring and winter wheat lines. In the winter wheat cultivars TDC (Triple Dirk C, *vrn-A1vrn-B1vrn-D1*) and JH9 (Jinghua 9, *vrn-A1vrn-B1vrn-D1*), *VAS* increased distinctly at 14 days of vernalization (supplemental Figure 1A). By contrast, the *VAS* transcript was not detected in the spring wheat cultivars CS (*vrn-A1vrn-B1Vrn-D1*) and TDB (*vrn-A1Vrn-B1vrn-D1*) (supplemental Figure 1B). This result suggests that *VAS* is found specifically in winter wheat. To determine whether *VAS* is generally induced by cold exposure in winter wheat, its expression was assessed in 106 accessions of wheat cultivars and land-races from a core germplasm collection in China (Zhang, et al., 2008). Notably, the *VAS* transcript was not detected after vernalization treatment in any spring habit wheat, such as CS, SS, TDB, W15A, and W11B, whereas it appeared during early vernalization treatment in most winter habit wheat accessions, such as TDC, W7A (*vrn-A1vrn-B1vrn-D1*), KN199 (*vrn-A1vrn-B1vrn-D1*), JD1 (*vrn-A1vrn-B1vrn-D1*), and JH9 (Figure 1A and 1B and supplemental Figure 2A and 2B). Further sequence analysis showed that all 106 materials tested possessed the transcriptional start site and the proper GT-AG splicing sites at the *TaVRN1* gene, regardless of their winter or spring habit (Figure 1B and supplemental Figure 2C). However, alignment of the *VAS* sequence amplified from vernalized winter wheat (KN199) showed that all of the *VAS*-containing clones sequenced were from a sub-genome in KN199 (supplemental Figure 3). Thus, *VAS* may be produced specifically in wheat with a winter habit, but not in spring wheat, possibly because it is preferentially produced from the winter allele *TaVRN-A1*, which is absent in most spring wheat.

VAS RNA consists of 662 nucleotides, initiates from the same transcriptional start site as *TaVRN1*, contains the intact first exon, and spans part of the first intron, ending within the "critical region" (Figure 1C–1E and supplemental Figure 4A). *VAS* is a novel alternative splicing transcript of *TaVRN1*, which is distinct from the normal transcript, possibly with two potential coding products based on the sense strand ranging from amino acids 13 to 154 (supplemental Figure 4B). Sequence scanning of the A/B/D sub-genome suggested that all three sub-genomes have the potential to produce *VAS* (Figure 1F). RT–qPCR results showed that increased levels of *VAS* were clearly observed during cold exposure, with maximal expression at 21 days of cold exposure, followed by a decline. *VAS* expression returned to the pre-vernalized level after the return to normal temperature at any time point during cold exposure (Figure 1G). This transient induction of *VAS* was distinct from the expression profile of *TaVRN1*, which continuously increased during vernalization and remained high, even after a return to normal temperature (Figure 1H). This pattern suggests that *VAS* may play an important role in the early stage of vernalization.

VAS functions as an lncRNA to promote wheat flowering

To explore the biological importance of *VAS*, the full length of *VAS* was driven by the constitutive ubiquitin promoter and transformed into KN199, a major winter cultivar in the Northern areas of China. The *VAS-OE* transgenic plants showed earlier shoot apical meristem transformation, significantly reduced heading time, and fewer tillers compared with the wild type under different periods of cold exposure (Figure 2A and supplemental Figure 5A–5D). The abundance of *TaVRN1 and FT1* transcripts was increased in *VAS-OE lines compared with KN199*, whereas the expression of the flowering repressor *VRN2* was reduced (supplemental Figure 5E–5G). These results indicated that *VAS* regulated *TaVRN1* to accelerate flowering in winter wheat.

To clarify whether *VAS* functions as a coding gene or an lncRNA, we overexpressed two "artificially mutated" versions of *VAS*, with the start codon "ATG" of the predicted long open reading frame of *VAS* mutated to "TTG" or "ATGC," in KN199 (supplemental Figure 6). *VAS*-TTG-OE and *VAS*-ATGC-OE transgenic lines showed earlier flowering compared with the wild type, similar to the *VAS-OE* transgenic lines (Figure 2B and 2C). The transcription levels of *TaVRN1* and *FT1* exhibited similar patterns in *VAS-TTG*-OE and *VAS-ATGC*-OE as in *VAS*-OE (Figure 2D–2F). This suggests that the *VAS* transcript, rather than the encoded product, was functional. Furthermore, two polypeptide antibodies for the predicted "VAS" protein with 154 amino acids were developed to determine whether there was a translation product of *VAS in planta*, but no target protein was detected in winter wheat before or with vernalization treatment (supplemental Figure 7A–7C). Collectively, these results suggest that *VAS* works as an lncRNA to promote vernalization-mediated flowering by accelerating the activation of *VRN1*.

VAS binds with the transcription factor RF2b during vernalization

How does the lncRNA *VAS* affect *TaVRN1* transcription? lncRNAs can serve as molecular structures to facilitate the targeting of protein complexes to specific genomic loci (Heo and Sung, 2011; McHugh et al., 2015). To identify potential factors associated with *VAS*, a ChIRP-MS (chromatin isolation by RNA purification associated with mass spectrometry) assay was conducted (Kim et al., 2017). Six probes labeled with biotin were designed based on the *VAS* sequence (Figure 3A and 3B). Vernalized shoot tips were used for ChIRP. The qPCR result demonstrated that *VAS*, rather than *TaVRN1*, was enriched in the immunoprecipitated (IP) fraction, confirming the robustness of our ChIRP assay (Figure 3B). The co-precipitated proteins were identified by mass spectrometry. They included transcription factors such as RF2b (a basic leucine zipper [bZIP] transcription factor) and NAC domain proteins, two protein kinases such as NEK4 (associated with meiosis and DNA damage), the shear factor protein SF2 (associated with pre-RNA variable splicing), and so on (Figure 3C). These proteins may be associated with variable splicing and transcriptional regulation of *TaVRN1*. Motif analysis showed that *VAS* contains putative bZIP binding motifs, such as Box II, Sp1, and G-box. We therefore focused on RF2b, which is a bZIP transcription factor. Indeed, an RIP-qPCR assay confirmed that RF2b bound to *VAS* during vernalization (Figure 3D). The RF2b-*VAS* association peaked at 20 days of cold exposure (V20), then

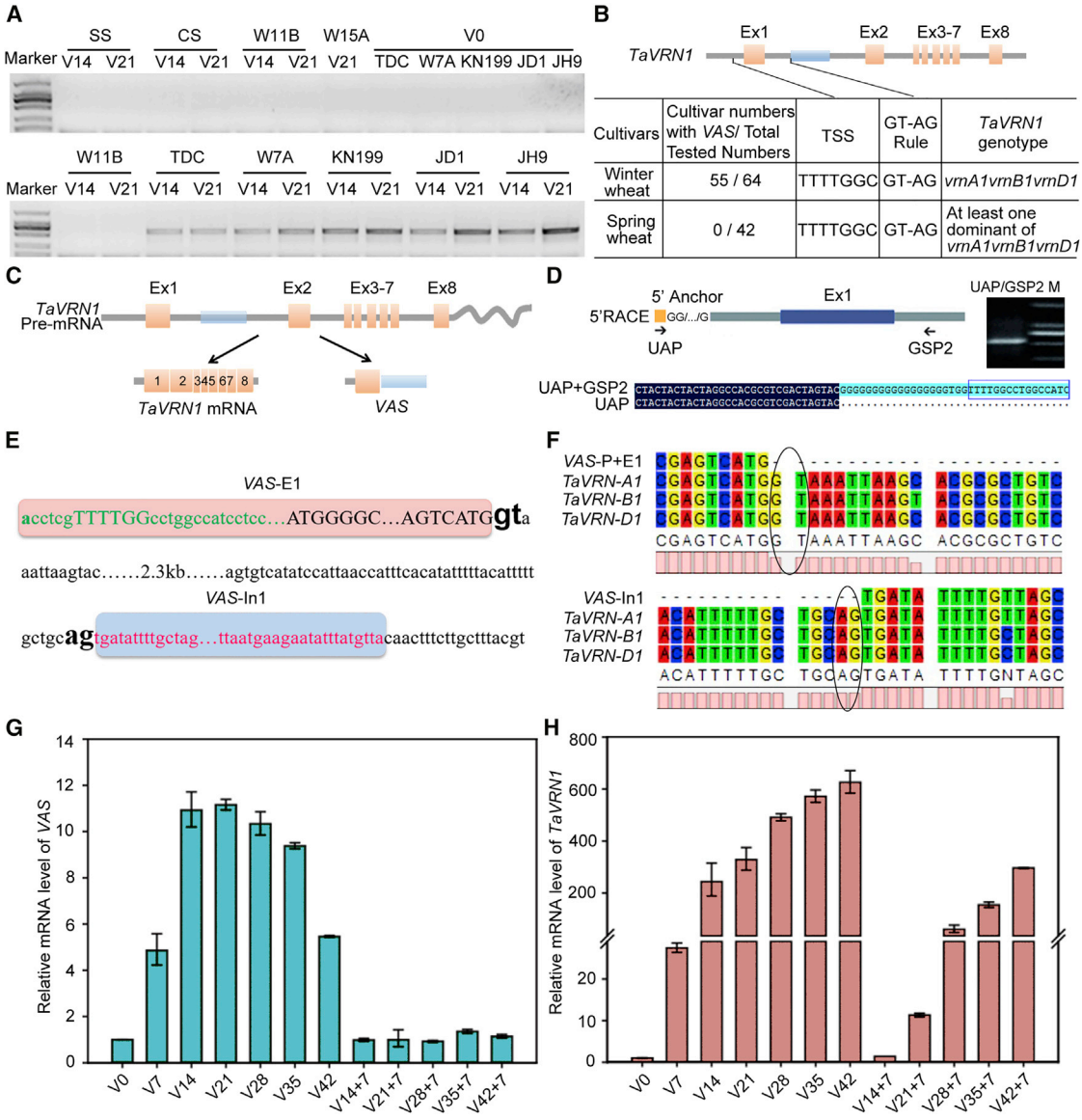

Figure 1. Identification of the novel transcript *VAS* induced by vernalization in winter wheat.

(A–F) (A) The expression of *VAS* in different spring or winter wheats was detected by PCR. CS, Chinese Spring; TDC, Triple Dirk C; KN199, Kenong 199; JD1, Jingdong 1; JH9, Jinghua 9. **(B)** The detection of *VAS* and the genotypes of *TaVRN1* in different winter and spring cultivar wheats. TSS, transcription start site; GT-AG rule, the splice sites at the exon-intron boundary. **(C)** *TaVRN1* pre-mRNA produces two transcripts, *TaVRN1* and *VAS*, through alternative splicing. **(D)** A 5′ RACE assay confirmed the TTTTGGC site as the transcriptional start site of *VAS* as well as *TaVRN1*. **(E)** Splice sites at the exon1–*VAS*–intron1 boundary. The dark and bold gt/ag stands for the splice sites. **(F)** The GT/AG splice sites in *TaVRN-A1*, *TaVRN-B1*, and *TaVRN-D1*. **(G and H)** The relative expression of *VAS* **(G)** and *TaVRN1* **(H)** in response to different vernalization durations (data were first normalized to the housekeeping gene *Actin*, then normalized to V0 plants). Data shown are means ± SD, $n = 3$. V0, no vernalization; V14, vernalized for 14 days; V14 + 7, vernalized for 14 days followed by growth at room temperature (25°C) for 7 days.

declined during the late period of vernalization (V30), suggesting that the RF2b-*VAS* interaction is transient, especially during early vernalization. Thus, RF2b was a potential factor associated with *VAS* during vernalization.

RF2b and RF2a form a heterodimer to promote *TaVRN1* expression and accelerate flowering

RF2b generally interacts with RF2a to form a heterodimer that functions in transcriptional regulation (Liu et al., 2007). Both RF2b and RF2a are located in the nucleus, overlapped with H2A (supplemental Figure 8). Wheat RF2b was shown to interact with RF2a to form heterodimers via yeast two-hybrid and luciferase (Luc) complementation experiments (Figure 4A and 4B). Notably, a DNA electrophoretic mobility shift assay (EMSA) showed that RF2b bound to the promoter of *TaVRN1* at the Sp1 motif (Figure 4C). To test their transcriptional regulation activity, *RF2b* and *RF2a* coding sequences were fused in frame with the GAL4 DNA binding domain (BD) coding sequence in the effector vector (Figure 4E).

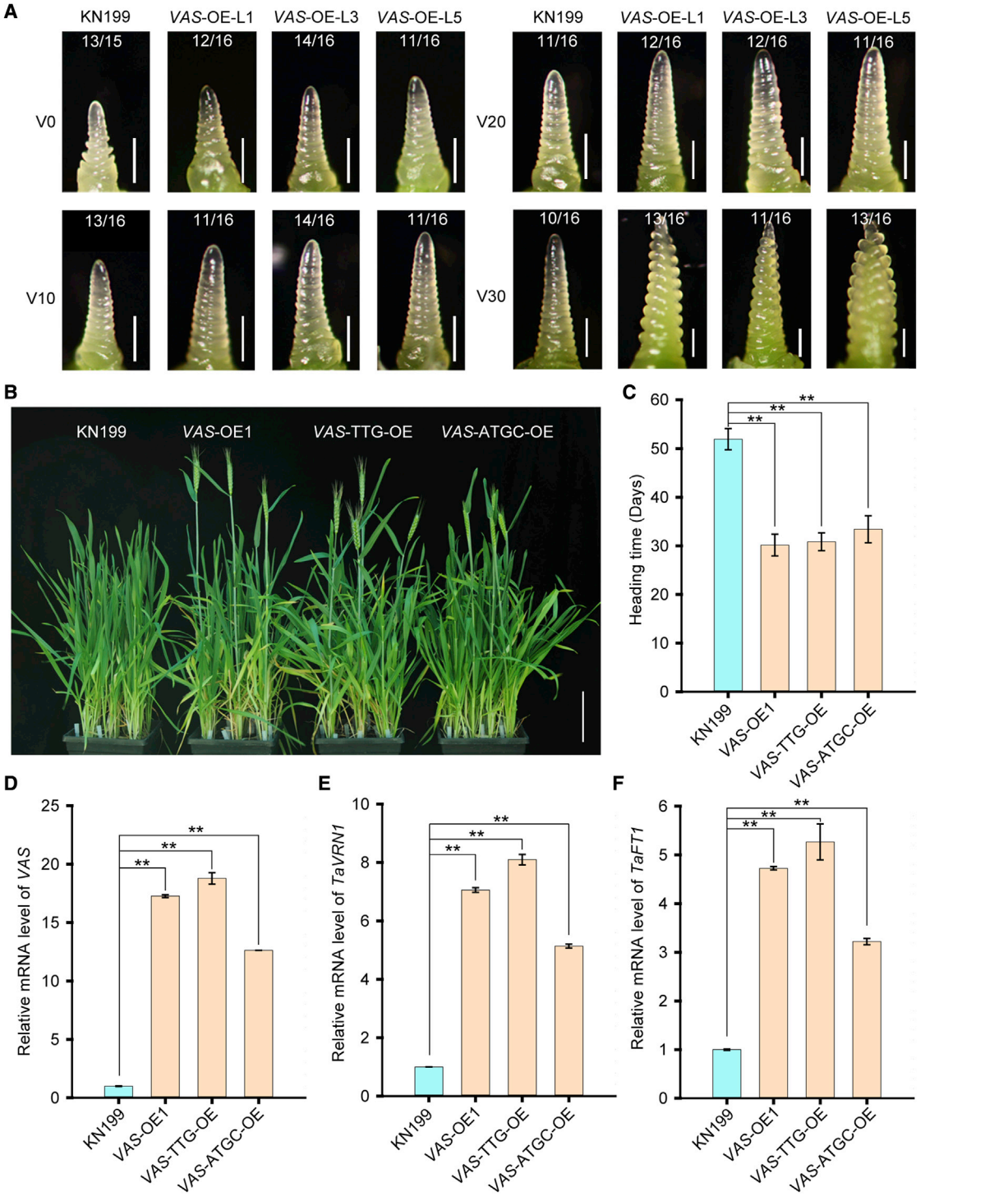

Figure 2. *VAS* functions as an lncRNA to promote flowering in winter wheat.

(A) The shoot apical morphology of winter wheat KN199 and the transgenic plants *VAS*-OE-L1, L3, and L5 (45 days after germination [DAG]) with different durations of cold exposure (V0, V10, V20, and V30). The proportion shows the fraction of dissected plants whose stage was similar to that of the displayed plant or the following stage. V0, V10, V20, and V30: no vernalization and vernalized for 10, 20, or 30 days. Scale bars correspond to 0.5 mm.

(B) The overexpression transgenic lines (*VAS*-OE-L1, *VAS*-TTG-OE, and *VAS*-ATGC-OE) show earlier flowering than wild-type KN199.

(C) Heading time (60 DAG) of *VAS*-OE transgenic wheat and wild-type KN199 (Kongnong199) vernalized for 20 days in the greenhouse. Data are means ± SD of 24 plants for each line; $^{**}P < 0.01$, two-tailed *t-test*.

(D–F) Relative expression of *VAS* **(D)**, *TaVRN1* **(E)**, and *TaFT1* **(F)** in *VAS*-OE transgenic wheat and wild-type KN199 (data were first normalized to the housekeeping gene *Actin*, then normalized to KN199 plants). Data shown are means ± SD, $n = 3$; $^{**}P < 0.01$, two-tailed *t-test*.

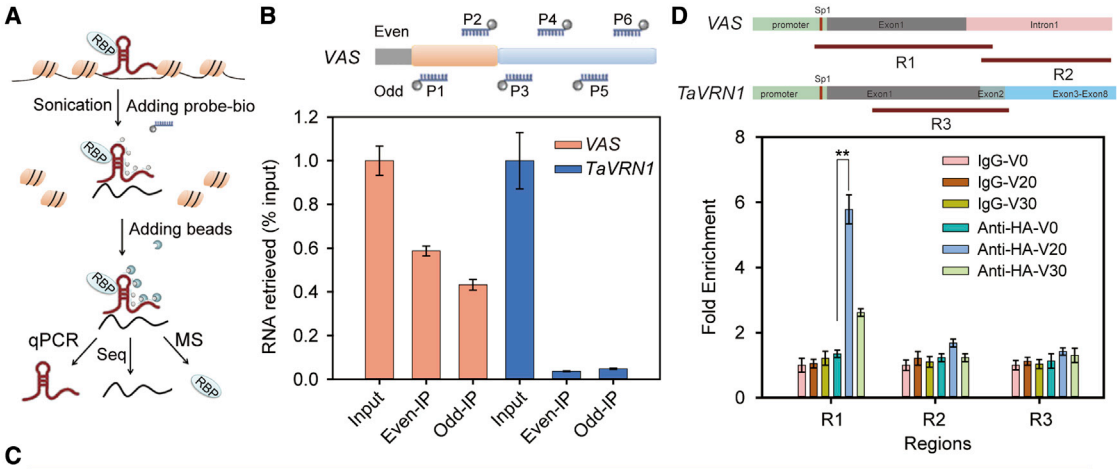

C

Gene Number	Description	Coverage(%)
TraesCS5A02G308400	Transcription factor RF2b	30
TraesCS1A02G275900	NAC-domain protein	7
TraesCS5D02G512100	Chaperone protein dnaJ	2
TraesCS5B02G177500LC	NIMA-related kinase 4	25
TraesCS1A02G530600LC	Endonuclease/exonuclease/phosphatase protein	11
TraesCS7D02G087500	Early nodulin 93	6
TraesCS4D02G168700	splicing factor-like protein	4
TraesCS7B02G702400LC	F-box protein	3
TraesCSU02G089600LC	Protein kinase family protein	4
TraesCS6B02G222900LC	Sister chromatid cohesion protein PDS5A	8
TraesCS5A02G576700LC	Transposon Ty3-I Gag-Pol polyprotein	14

Figure 3. Identification of *VAS* binding proteins by ChIRP-MS.
(A–D) (A) Schematic diagram of the ChIRP method; **(B)** Diagram of the designed biotin probe; enrichment of *VAS* was detected. **(C)** Detailed information on proteins identified by *VAS*-ChIRP-MS. **(D)** RIP-qPCR assay to analyze the binding of TaRF2b to *VAS*. The relative locations of each region, R1 to R3, are indicated in the upper panel. Immunoglobulin G was used as a control. Data are means ± SD, $n = 3$; $^{**}P < 0.01$, two -tailed *t*-test. V0, V10, V20, and V30: non-vernalization or vernalized for 10, 20, or 30 days.

Transcriptional activity assays showed that RF2b itself could hardly activate the GUS reporter, but RF2a and RF2a-RF2b activated the GUS reporter 3.5-fold more than the BD vector alone (Figure 4E), indicating that RF2a, rather than RF2b, has transcription activation activity. This observation was further confirmed by β-galactosidase activity in yeast (Figure 4D). These results suggest that the *VAS*-associated protein RF2b may recognize the promoter region of *TaVRN1* via the Sp1 motif, later activating its transcription through the formation of a heterodimer with RF2a.

To evaluate the function of RF2b in the vernalization response, *RF2b*-tagged hemagglutinin (HA) overexpression transgenic lines and the CRISPR mutants *tarf2b-1* and *tarf2b-2* were generated in the KN199 background (supplemental Figure 9). Sequencing of the gRNA target regions confirmed that the *tarf2b* CRSIPR mutants had several nucleotide deletions in all three subgenomes, which destroyed the bZIP domain of the protein product in *tarf2b-1* and *tarf2b-2* (supplemental Figure 9C). *RF2b*-OE lines exhibited accelerated flowering and reduced heading time compared with KN199, whereas the *tarf2b* mutants exhibited delayed flowering (Figure 5A–5C and supplemental Figure 10). The transcription patterns showed that *RF2b* expression was significantly higher in *RF2b*-OE than in KN199. The transcription of *TaRF2b* in *tarf2b-1* mutants was similar to that in KN199 (Figure 5D). *TaVRN1* also showed higher transcription in the *RF2b*-OE transgenic lines and lower transcription in the *tarf2b-1* mutant plants compared with KN199 (Figure 5E), whereas the transcription of *VAS* did not differ among KN199, *RF2b*-OE, and *tarf2b-1* mutant plants (Figure 5F). The absolute transcript amounts of *RF2a* and *RF2b* in wheat showed that the expression of *RF2a* was 15–25 times higher than that of *RF2b* during vernalization. This result suggested that there were enough RF2a proteins to be recruited by overexpressed of RF2b into more RF2a-RF2b complexes with transcriptional activation activity (Figure 4F and 4G). Overall, *VAS* binding to RF2b may accelerate wheat flowering by promoting the transcription of *TaVRN1*, together with RF2a.

Binding of RF2b to *TaVRN1* during vernalization is associated with *VAS* and a conformational change in the *TaVRN1* gene

To determine whether the binding of RF2b to the promoter of *TaVRN1* is associated with *VAS*, *RF2b-HA* overexpression transgenic wheat plants with or without vernalization treatment were

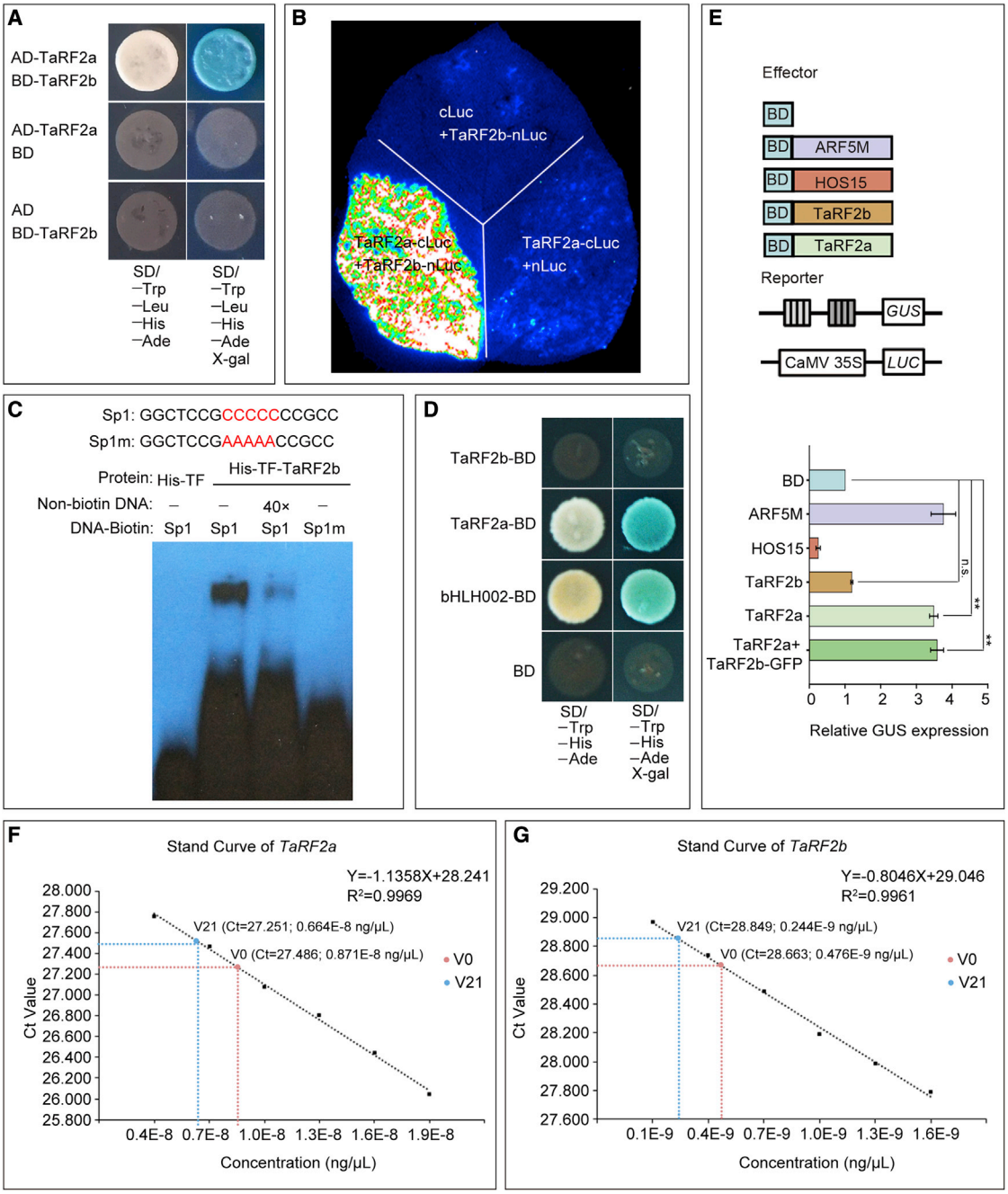

Figure 4. TaRF2b and TaRF2a form a heterodimer to promote transcription.

(A and B) Y2H assay and luciferase fluorescence complementation assay to confirm the interaction between TaRF2b and TaRF2a.

(C–E) (C) An EMSA assay to analyze the binding of TaRF2b to the Sp1 motif in the *TaVRN1* promoter. The competitor probe was added in 40-fold molar excess of labeled probes. **(D)** Analysis of TaRF2b and TaRF2a transactivation activity in yeast; bHLH002 was used as a positive control. **(E)** Transcriptional activity assays in *Arabidopsis* protoplasts. The effector plasmids encode BD-TaRF2b and BD-TaRF2a fusion proteins, which bind to the promoter in the reporter plasmid. *CaMV35S::LUC* was used as an internal control. ARF5M and HOS15 were used as positive and negative controls, respectively. Data are means ± SD, $n = 3$; $^{**}P < 0.01$, two-tailed *t-test.* n.s., not significant.

(F and G) The absolute transcript amount of *TaRF2a* **(F)** and *TaRF2b* **(G)** in wheat with or without vernalization treatment. V0, no vernalization; V21, vernalized for 21 days.

used to perform a chromatin immunoprecipitation (ChIP) assay with an anti-HA antibody (Figure 6A). The results demonstrated that the R2 region containing the Sp1 motif sequence was more highly enriched in vernalized wheat plants (Figure 6A). Moreover, qRT–PCR analysis indicated that the transcription level of *RF2b* in *RF2b-HA-OE* transgenic wheat plants was significantly higher than that in wild-type KN199, with or without vernalization treatment (Figure 6B). By contrast, the transcript level of *TaVRN1* was significantly higher in *RF2b-HA*-OE transgenic wheat plants than in the wild type only after vernalization treatment, and

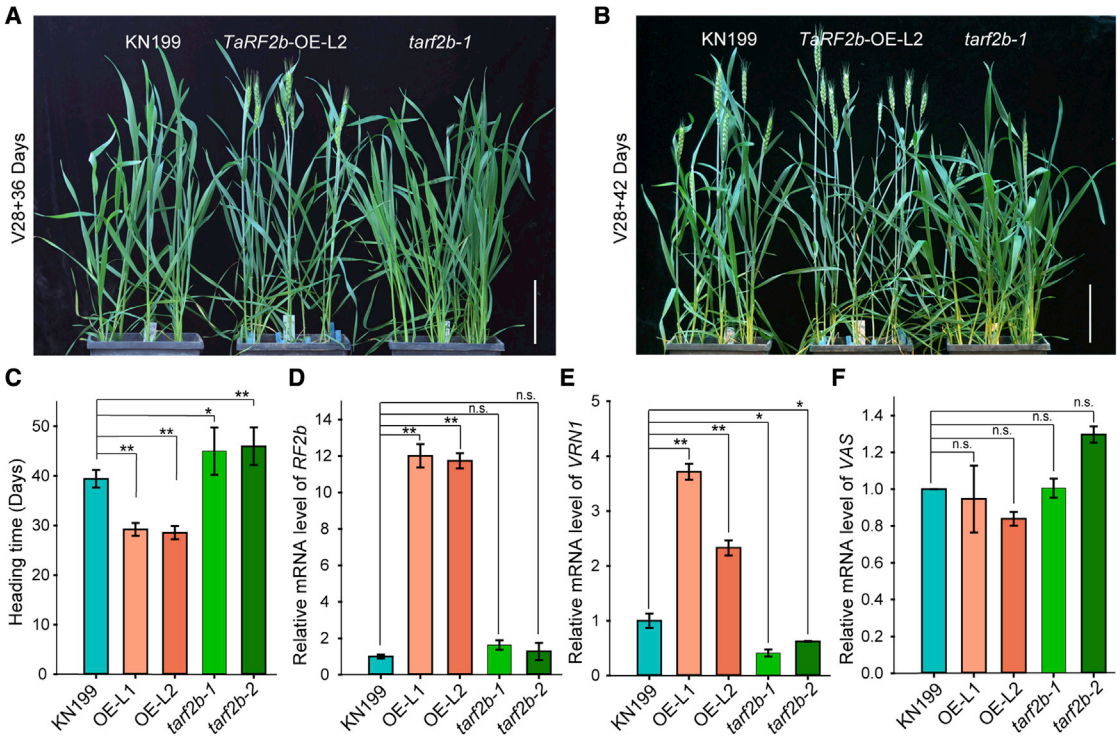

Figure 5. TaRF2b accelerates winter wheat flowering by regulating the expression of *TaVRN1*.

(A and B) Morphological phenotype of *TaRF2b*-OE and *tarf2b* transgenic wheat and wild-type KN199 with 28 days of vernalization and 36 days **(A)** and 42 days **(B) of growth** in the greenhouse.

(C) Heading time of *TaRF2b*-OE and *tarf2b* transgenic wheat and wild-type KN199. Data are means ± SD of 25 plants for each line. $^{**}P < 0.01$, $^{*}P < 0.05$, two-tailed *t-test*.

(D–F) Relative expression of *TaRF2b* **(D)**, *TaVRN1* **(E),** and *VAS* **(F)** in *TaRF2b*-OE and *tarf2b* transgenic wheat and wild-type KN199 wheat. Data were first normalized to the housekeeping gene *Actin*, then normalized to KN199 plants. Data shown are means ± SD, $n = 3$; $^{**}P < 0.01$, $^{*}P < 0.05$, two-tailed *t-test.* n.s., not significant.

vernalization treatment significantly increased the transcript level of *VAS* relative to non-vernalized plants (Figure 6C and 6D). These results suggested that the effect of RF2b on *TaVRN1* transcription was associated with *VAS* transcription.

The ChIP-qPCR results suggested that RF2b could not bind to the promoter of *TaVRN1* before vernalization (Figure 6A), hinting that the *TaVRN1* promoter region may have a conformational structure that conceals the RF2b binding site. To test this hypothesis, a chromosome conformation capture (3C) assay was performed. Winter wheat was exposed to various vernalization treatments (V0, V10, V20, and V30). Three primers in the promoter of *TaVRN1* and five primers in intron1 of *TaVRN1* were designed to detect juxtaposed regions in chromosome loops at the *TaVRN1* position (Figure 6E). PCR analysis of 3C samples from different vernalization treatments using different primers showed that *TaVRN1* formed a loop structure at the P2/I4 position that contained the complete *VAS* sequence. This loop gradually disappeared during vernalization (Figure 6F). The result of 3C-qPCR also showed that the loop structure nearly disappeared at 20 days of vernalization or in the late period of vernalization (V30) (Figure 6G). Further qPCR assays indicated that the opening loop was correlated with a marked increase in *TaVRN1* transcripts and a decrease in *VAS* transcripts (Figure 6H). In general, *TaVRN1* transcription increased, possibly owing to the release of the RF2b binding motif Sp1 along with the gradually opening loop during vernalization.

DISCUSSION

Wheat, a worldwide cereal grain, shows genetic variation in day-length sensitivity and vernalization requirement (Steinfort et al., 2017). Allelic variation at the *TaVRN1* locus is a main determinant of the vernalization requirement for winter or spring growth habit (Fu et al., 2005). But how *TaVRN1* is gradually induced during the vernalization process is not well understood. Here, we identified *VAS*, a novel alternative splicing transcript of Ta*VRN1* that functioned as an lncRNA to accelerate wheat flowering (Figures 1, 2 and supplemental Figure 5). *VAS* was induced by low temperature and peaked at 21 days of vernalization, suggesting that *VAS* functioned to activate the transcription of *TaVRN1* at the early period of vernalization (Figure 1). Detection of *VAS* in 106 accessions suggested that *VAS* may mediate the winter habit of wheat (Figure 1 and supplemental Figure 2). All of the *VAS* sequences derive mainly from the A sub-genome in KN199 (supplemental Figure 3), and *VAS* may be preferentially produced mainly from *TaVRN-A1*. The *VAS* sequence contains a partial promoter, an intact exon1, and a partial intron1 of *TaVRN1* (Figure 1). The intron1 portion in *VAS* derives mainly from the ''critical region'' of *TaVRN1*, which is largely deleted in spring alleles. It may be

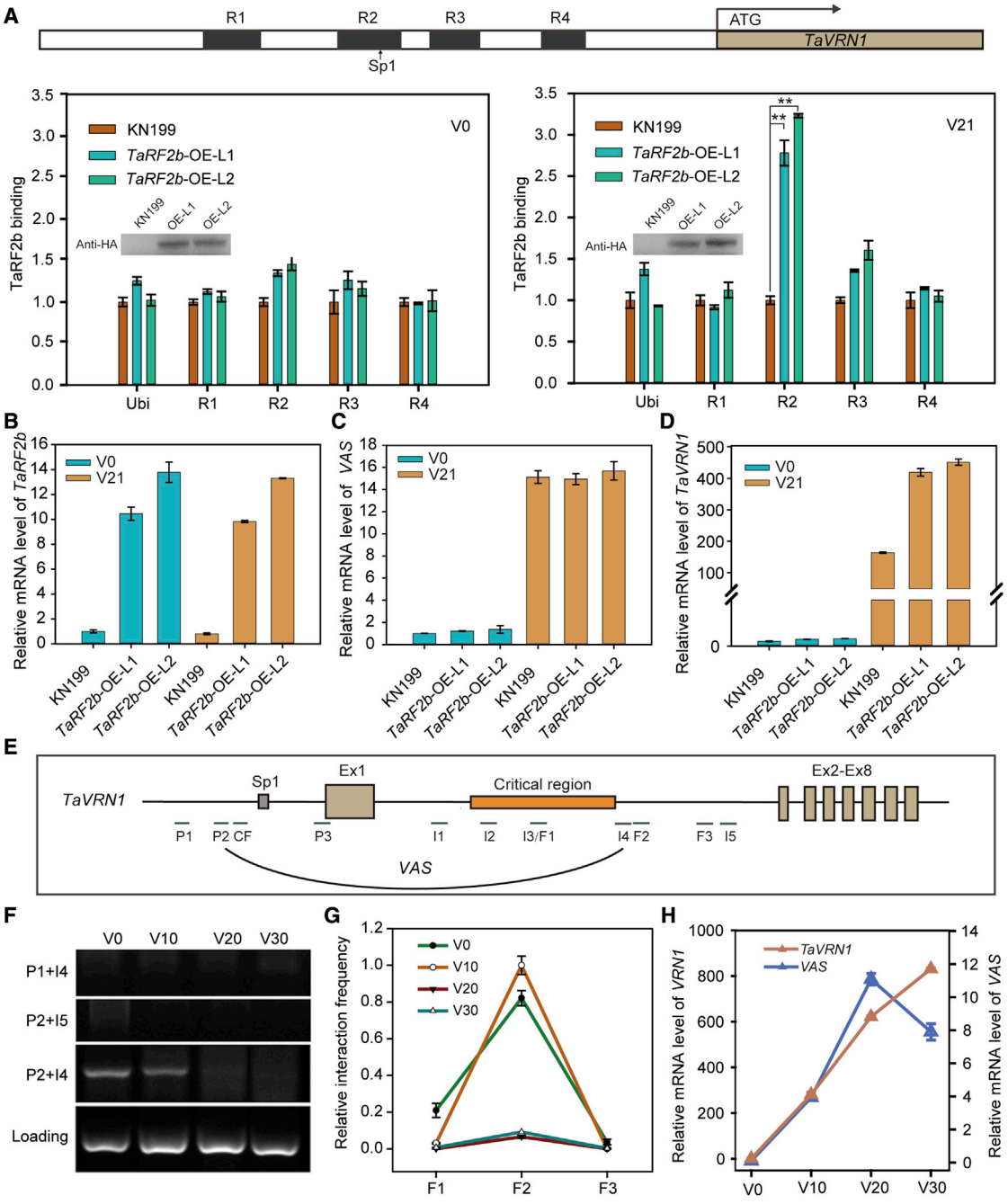

Figure 6. Binding of TaRF2b at the *TaVRN1* promoter is associated with the expression of *VAS* and breakage of a genic loop during the vernalization process.

(A) ChIP-qPCR assay of different vernalized sample apices to show the relative binding strength of TaRF2b-HA to different regions in the *TaVRN1* promoter. The relative locations of each region, R1 to R4, are indicated in the upper panel. The ubiquitin (Ubi) promoter was used as a control. Data are means ± SD, $n = 3$. $^{**}P < 0.01$, two-tailed *t-test*. The immunoblots show the RF2b-HA protein in the transgenic plants.

(B–D) Relative expression of *TaRF2b* **(B)**, *VAS* **(C),** and *TaVRN1* **(D)** in *TaRF2b*-OE transgenic wheat and wild-type KN199 wheat with or without vernalization. Data were first normalized to the housekeeping gene *Actin*, then normalized to KN199 plants. Data shown are means ± SD, $n = 3$. V0, no vernalization; V21, vernalized for 21 days.

(E and F) (E) Strategy for mapping juxtaposed regions in chromosome loops at the *TaVRN1* locus in winter wheat; **(F)** PCR analysis of 3C samples from different vernalized sample apices using the P1+I4, P2+I5, and P2+I4 primers shown in **(E)**.

(G) The 3C-qPCR assay quantified the relative interaction frequency between the *TaVRN1* promoter (P2) and intron1 regions (F1, F2, and F3). The position of each primer is shown in **(E)**; the cloned naked *TaVRN1* DNA was used for calibration.

(H) The expression of *TaVRN1* and *VAS* in different vernalized, devernalized, or revernalized samples. V0, V10, V20, and V30 indicate no vernalization or vernalization for 10, 20, or 30 days.

that *TaVRN1* already produced from the spring allele (e.g., *TaVRN-B1* or *TaVRN-D1*) inhibits the expression of *VAS* from the winter allele in spring wheat by promoting its own expression.

In *Arabidopsis*, the lncRNAs *COLDAIR*, *COOLAIR*, and *COLDWRAP* from the sense or antisense strand of *FLC* regulate its silencing by recruiting the PRC2 complex (Helliwell et al., 2011; Heo and Sung, 2011; Sun et al., 2013; Csorba et al., 2014; Marquardt et al., 2014; Kim et al., 2017; Kim and Sung, 2017). In wheat, by contrast, the transcriptional level of *TaVRN1* is kept low prior to low-temperature exposure thanks to the large amount of H3K27me3 modification occurring at the *TaVRN1* locus. Upon vernalization, the H3K27me3 modification is replaced by H3K4me3 at the *TaVRN1* locus, resulting in the high expression of *TaVRN1* (Xiao et al., 2014). This epigenetic regulatory mechanism is opposite to that of *FLC* in response to vernalization in *Arabidopsis* (Luo and He, 2020; Xu and Chong, 2018; Whittaker and Dean, 2017), suggesting that the function of *VAS* may be distinct from that of the lncRNAs that regulate *FLC* silencing. In addition, our data suggest that the lncRNA *VAS* can facilitate binding of the RF2a-RF2b heterodimer to the Sp1 motif in the *TaVRN1* promoter to promote the transcription of the normal *TaVRN1* transcript during vernalization (Figures 3, 4, 5, and 6). These results may highlight a novel regulatory mechanism by which an lncRNA regulates vernalization-induced flowering in plants.

The RF2b-RF2a complex has not previously been shown to contribute to regulation of vernalization-mediated flowering in wheat, although RF2b and RF2a regulate the symptom development of rice tungro disease (Yin et al., 1997; Dai et al., 2003, 2004, 2008; Liu et al., 2007; Ordiz et al., 2010). Overexpression of *RF2b* can significantly accelerate wheat flowering and promote the high expression of *TaVRN1* (Figure 5). Although RF2b showed little transcription activation activity *in vitro*, overexpression of *RF2b* can facilitate more binding of RF2b protein to the released *TaVRN1* promoter and recruit more of the partner, RF2a. This physical interaction generates strong transcription activation activity. The expression of *RF2a* is higher than that of *RF2b* during vernalization, suggesting that more RF2a-RF2b complexes can be formed when RF2b is overexpressed (Figure 4F and 4G). More RF2b-RF2a complexes reside at the promoter of *TaVRN1* and activate its transcription, resulting in the accumulation of *TaVRN1* mRNA and thereby causing accelerated wheat flowering.

A potential higher order and/or condensed chromatin structure in the sequence of the *TaVRN1* gene may have blocked the regulatory regions, which were gradually released during vernalization. Before vernalization, the transcriptional level of *TaVRN1* in wheat is very low, perhaps in part because the binding of some transcription factors to the *TaVRN1* promoter relies on vernalization. Our data suggested that vernalization induced the binding of RF2b to the Sp1 motif in the *TaVRN1* promoter (Figure 6A). The P2 motif in the *TaVRN1* promoter and the I4 motif in *TaVRN1* intron1 can adhere together to form a chromosome loop at the *TaVRN1* locus before vernalization, and this is gradually opened during vernalization (Figure 6E and 6F). This loop structure contains multiple regulatory regions, such as the VRN box, the CArG box, and the Sp1 motif. Levels of *VAS* and *TaVRN1* transcripts in samples exposed to different durations of vernalization suggested that vernalization treatment promoted the transcription of both *TaVRN1* and *VAS* in the early period of vernalization (Figure 6H). After sufficient vernalization, the transcription of *TaVRN1* increased dramatically, but the transcription of *VAS* began to decline (Figure 6H). This indicated that the conformational loop structure at the *TaVRN1* gene was disrupted by vernalization treatment. The opened loop structure potentially released the regulatory regions of *TaVRN1*, facilitating the binding of RF2b to the Sp1 motif and the binding of VRT2 to the CArG box in the *TaVRN1* promoter. Binding of these proteins to the *TaVRN1* promoter further activated *TaVRN1* transcription (Figure 6A and 6D) (Xie et al., 2019). The formation of the loop structure may be associated with various histone modification switches and a conformational structure change. The chromatin cohesion protein PDS5A and a degradation-related F box protein were also identified by *VAS*-ChIRP-MS (Figure 3C). This result suggests that *VAS* may function in regulating the disruption or formation of the chromatin structure together with some epigenetic mediators during vernalization, apart from the VAS-RF2b-mediated vernalization module (Figure 3). In the future, it will be worthwhile to explore further epigenetic regulatory mechanisms by which *VAS* participates in the formation or disruption of the loop structure before or after vernalization, as well as the relationship between the loop structure and *VAS*.

In summary, the novel lncRNA *VAS* and the Sp1 motif are contained in a loop structure at *TaVRN1* before vernalization in winter wheat. During the early period of vernalization, *TaVRN1* produces more *VAS* lncRNA. Subsequently, the disrupted loop structure facilitates *VAS* recruitment of an RF2b-RF2a complex that binds the Sp1 motif, thereby promoting *VRN1* transcription and accelerating flowering initiation in later vernalization (Figure 7). Our study reveals a new mechanism by which an lncRNA regulates wheat vernalization and flowering, providing theoretical guidance for wheat molecular breeding.

MATERIALS AND METHODS

Growth conditions and vernalization treatment

Seeds of winter wheat and spring wheat (*Triticum aestivum* cv. JD1, JH9, TDC, etc. and CS, TDB, etc.) were surface sterilized in 2% NaClO for 20 min, then rinsed overnight with flowing water. Seeds were germinated on moist filter paper at 4°C in the dark for 7, 14, 21, 28, 35, or 42 days (V7, V14, V21, V28, V35, and V42) and then grown at room temperature for 1 week (V14 + 7…, V42 + 7) or at 25°C for 3 days (V0). Wheat plumules from these samples were used to extract RNA for RT–PCR and RT–qPCR. Seeds of *VAS* or *TaRF2b* transgenic lines were surface sterilized and rinsed overnight with flowing water. The seeds were then germinated on moist filter paper at 4°C in the dark for 20 days (V20) or at 25°C for 3 days (V0). The plants were transferred to soil and grown in a greenhouse (20°C–22°C, 16-h light/8-h dark). For natural vernalization, seeds without cold exposure were sown in the field at the Institute of Botany, CAS, Beijing, China at the beginning of October each year. They experienced natural vernalization during the winter and flowered the following spring.

Wheat transformation

For overexpression analysis, the full-length cDNA of *TaRF2b* and the whole sequence of *VAS* were inserted into pUN1301, a binary vector that carries the maize ubiquitin promoter. For knockout mutant analysis, the CRISPR-Cas9 system was used to generate the knockout mutant. The single mutant of *TaRF2b*^{ko} (sgRNA designed in exon2) was generated under the *TaU6* wheat promoter. *Agrobacterium tumefaciens* (strain EHA105)-mediated transformation was used to introduce the constructs into the Chinese winter wheat (*T. aestivum*) cultivar KN199.

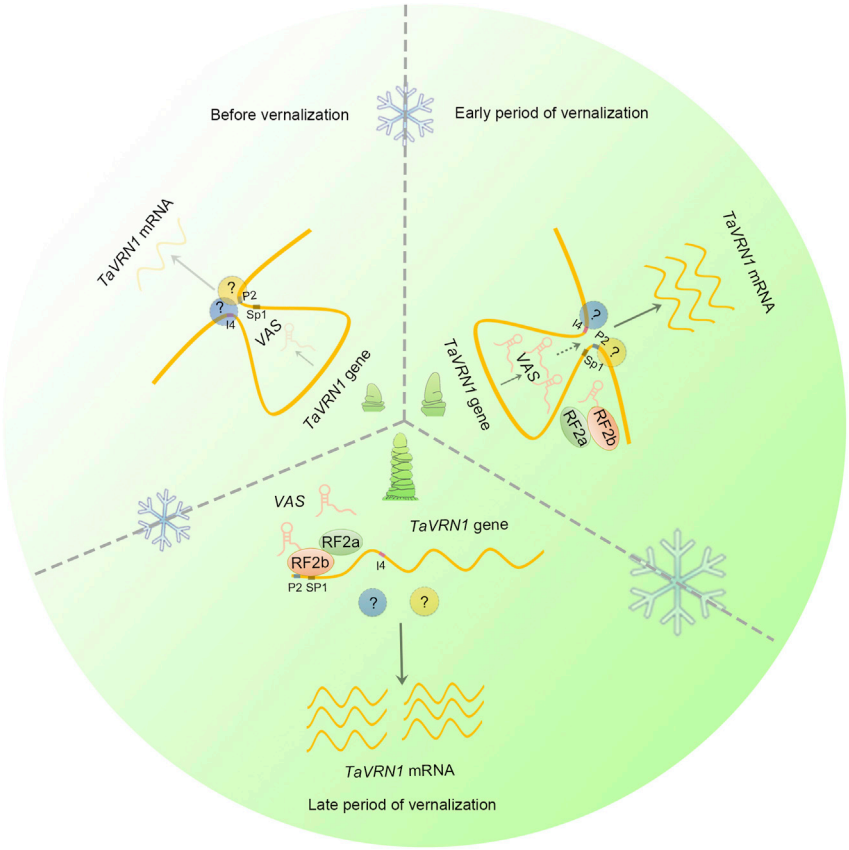

Figure 7. model showing how *VAS*-regulates *TaVRN1* transcription during vernalization in wheat.

TaVRN1 forms a loop structure at position P2/I4 under the action of some proteins before vernalization in winter wheat, which contains the complete *VAS* sequence. During the early period of vernalization, *TaVRN1* produces more *VAS* transcripts. Subsequently, *VAS* promotes the transcription of normal *TaVRN1* transcripts by recruiting proteins, such as the transcription factor TaRF2b, which binds the Sp1 motif of the *TaVRN1* promoter, together with TaRF2a. During vernalization, the disruption of the *TaVRN1* loop structure formed by the P2 motif and the I4 motif facilitates binding of the TaRF2b-TaRF2a complex to the Sp1 motif, promoting the transcription of normal *TaVRN1* transcripts and accelerating flowering initiation.

Gene expression analysis

Plant total RNA was isolated using a TRIzol RNA Extraction Kit (Invitrogen) and treated with RNase-free DNase I (MBI Fermentas). A 2-μg aliquot of total RNA was used to synthesize cDNA using AMV reverse transcriptase (Promega). The cDNA was diluted 1:30 into 15 μl SYBR Green quantitative PCR Master Mix (Toyobo) according to the manufacturer's instructions. Quantitative RT–PCR was performed on Q5 (Invitrogen). The gene expression levels were normalized to that of *Actin*. Each experiment included three technical replicates and at least three biological replicates. The values represent means ± SD of three technical replicates, and primer sequences are provided in supplemental Table 1.

Western blot analysis

Total protein or nuclear fractions were extracted from wheat plumules with or without vernalization treatment and quantified by Bradford assay, then separated by denaturing polyacrylamide electrophoresis on 4%–12% SDS–PAGE gels and electroblotted onto polyvinylidene fluoride membranes. VAS potential protein was detected using anti-VAS antibody in Tris-buffered saline with Tween 20 buffer with 5% BSA at a 1/1000 dilution. Stabilized streptavidin–HRP conjugate (Thermo Scientific) was used for secondary detection at a 1/10 000 dilution, and SuperSignal West Dura substrate (Thermo Scientific) was used for signal detection.

Yeast two-hybrid analysis

Yeast two-hybrid analysis was performed according to the manufacturer's manual of the Matchmaker GAL4 Two-Hybrid System (Clontech). The prey plasmid, pGADT7-*TaRF2a*, was co-transformed with the bait plasmid, pGBKT7-*TaRF2b*, into *Saccharomyces cerevisiae* strain AH109. After culturing on synthetic medium plates (SD medium) lacking Trp and Leu (SD/-Trp/-Leu) at 30°C for 2 days, the transformants were transferred onto SD/-Trp/-Leu/-His/-Ade containing X-gal (5-bromo-4-chloro-3-indolyl-β-D-galactopyranoside) for blue color development.

Firefly Luc complementation imaging assays

The pairs of vectors (TaRF2b-nLuc/TaRF2a-cLuc, TaRF2b-nLuc/cLuc, and nLuc/TaRF2a-cLuc) were transformed into *Nicotiana benthamiana* leaves by *Agrobacterium*-mediated transformation for 48 h. Leaves were examined 2 days after transformation.

Subcellular localization

For RF2b and RF2a subcellular localization, 35S::RF2b-GFP and 35S::RF2a-GFP constructs were generated in pBI221. The plasmids were transformed into wheat protoplasts released from leaf sheaths of 10-day-old etiolated wheat seedlings by a polyethylene glycol-mediated transient expression system. The transformed protoplasts were observed using a fluorescence microscope (Leica TCS SP5), and images were analyzed with Image LAS-AF software.

RIP-qPCR

RIP was performed and modified as described previously (Xiao et al., 2014). In brief, 3 g of wheat plumules with different vernalization treatments were collected and crosslinked with 2% (v/v) formaldehyde. Plant material was ground and suspended in 15 ml of Honda buffer (0.44 M sucrose, 1.25% [w/v] Ficoll, 2.5% [w/v] dextran T40, 20 mM HEPES–KOH [pH 7.4], 10 mM $MgCl_2$, 0.5% [v/v] Triton X-100, 5 mM dithiothreitol, 1 mM phenylmethylsulfonyl fluoride [PMSF], and 1× plant protease inhibitors) supplemented with 8 units ml^{-1} RNase inhibitor and filtered through two layers of Miracloth (Calbiochem). Centrifugation was performed at 3000 *g* for 10 min at 4°C. The pellet was resuspended in 500 μl of nucleus lysis buffer (50 mM Tris–HCl [pH 8], 10 mM EDTA, 1% [w/v] SDS, 1 mM PMSF, and 1× plant protease inhibitors) plus 160 units ml^{-1} RNase inhibitor. Samples were sonicated and centrifuged, and the supernatant was transferred to fresh tubes. DNA concentrations were measured to ensure that nuclear protein concentrations were similar in all samples. Aliquots of 100 μl were prepared. The samples were then diluted 10-fold with ChIP dilution buffer (1.1% [v/v] Triton X-100, 1.2 mM EDTA, 16.7 mM Tris–HCl [pH 8], and 167 mM NaCl) plus 350 units ml^{-1} RNase inhibitor. IP was performed by adding 2 μl of HA antibody and 20 μl of protein A agarose/salmon sperm DNA (Upstate; 16157) prewashed three times with binding/washing buffer (150 mM NaCl, 20 mM Tris–HCl [pH 8], 2 mM EDTA, 1% [v/v] Triton X-100, 0.1% [w/v] SDS, and 1 mM PMSF) to the solution. Preimmune mouse serum was used as a negative antibody control. After incubating on a rotator for 3 h at 4°C, beads were washed four times with 1 ml of

binding/washing buffer plus 40 units ml^{-1} RNase inhibitor, and the protein–RNA complex was eluted with 50 μl of RIP elution buffer (100 mM Tris–HCl [pH 8], 10 mM EDTA, and 1% [w/v] SDS) plus 40 units ml^{-1} RNase inhibitor. Then the protein was degraded with proteinase K, and RNA was extracted with acidic phenol/chloroform and precipitated with ethanol supplemented with 3 M NaAc (pH 5.2) and 5 mg ml^{-1} glycogen (Ambion). The pellet was washed with 70% (v/v) ethanol, air dried, and dissolved in RNase-free water. The RNA sample was incubated with DNase I to digest the DNA contaminant.

For identification and quantification by RT–PCR, RNA samples were polyadenylated at 37°C for 30 min with 5 units of poly(A) polymerase (Takara). Poly(A)-tailed RNA was recovered by phenol/chloroform extraction and ethanol precipitation. A 5′ adapter (GeneRacer RACE ready cDNA kit; Invitrogen) was ligated to poly(A)-tailed RNA using T4 RNA ligase (Invitrogen), and the ligation products were recovered by phenol/chloroform extraction followed by ethanol precipitation. RT was performed using a GeneRacer Oligo(dT) primer (SuperScript III) with 200 units of SuperScript III reverse transcriptase (Invitrogen). The first-round PCR was performed for 22 cycles with GeneRacer 5′/3′ primers. The PCR products were separated on a 1% (w/v) agarose gel, and DNA smears from 200 to 800 bp were recovered and diluted 20-fold to be used as templates for the second-round of PCR with GeneRacer nested 5′/3′ primers. The PCR products were separated on a 1% (w/v) agarose gel, and DNA smears from 150 to 800 bp were recovered and diluted 50-fold to be used as templates for the detection of gene fragments with gene-specific primers. For quality checking and quantification, the genomic DNA served as a positive control for PCR, and input samples were used for equal loading.

RNA EMSA and DNA EMSA

TF-His-RF2b recombinant protein was expressed in the *Escherichia coli* BL21 (DE3) strain and purified using a nickel-affinity chromatography column. An EMSA assay was performed using a LightShift Chemiluminescent EMSA Kit (Thermo Fisher Scientific) according to the manufacturer's protocol with some previously described modifications. Oligonucleotides complementary to different motifs of the *TaVRN1* promoter were synthesized, annealed, and labeled using a Biotin 3′ End DNA Labeling Kit (Pierce). RNA probes labeling biotin were synthesized by Thermo Fisher. All probe sequences, including those for mutations, are listed in supplemental Table 1.

Transcription activity assays

The transcription activity assays were performed in transiently transformed *Arabidopsis* protoplasts as described previously (Guo et al., 2013). The DNA BD from GAL4 BD (amino acids 1–147) was used in this system. The effector region of the plasmids encoded BD-RF2b and BD-RF2a fusion proteins driven by the 35S promoter. The reporter plasmid GAL4(4X)-D1-3(4X)::GUS contains four tandem copies of the GAL4 DNA binding sites and four tandem copies of the constitutive D1-3 elements. Two known proteins, HOS15 and ARF5M, were used as the transcription suppression and activation controls, respectively. The GUS reporter and the Luc reporter were co-transformed with GAL4 BD-RF2b or BD-RF2a into *Arabidopsis* protoplasts. The 35S::Luc reporter was used as an internal control. Relative GUS activity was calculated (GUS/Luc) to determine transactivation activity. To observe the effect of RF2b on the transcriptional activity of RF2a, 35S::RF2b-GFP was co-expressed with BD-TaRF2a in *Arabidopsis* protoplasts in this assay system.

ChIRP assay

The ChIRP assay was performed according to the protocol from Magna ChIRP RNA Interactome Kits (Millipore) and from Kim et al. (2017) with some modifications. In brief, 3 g of vernalized wheat plumules were treated with 1% formaldehyde for protein–RNA–DNA crosslinking. The samples were ground, and the nuclei were extracted and sonicated to shear DNA. The chromatin was isolated with biotin probes for VAS using Streptavidin Magnetic Beads. The obtained protein–RNA–DNA complexes were processed for RNA isolation and protein isolation. Finally, the enriched RNA was analyzed by qPCR, and the enriched proteins were analyzed by MS.

Chromosome 3C assay

We used approximately 3 g of different vernalized wheat plumules for each round of the 3C assay. The harvested samples were ground with liquid nitrogen. The slurry was resuspended with nuclei isolation buffer (Hovel et al., 2012) supplemented with 2% formaldehyde. This was placed under vacuum immediately with the following settings: the vacuum rapidly switched ON and OFF 4 times, then vacuum for 15 min twice. Next, 1.334 ml of 2 M glycine (final concentration 0.125 M) were added to the tube, mixed by gently shaking, and vacuumed for 10 min to stop the crosslinking. The steps were generally performed according to the 3C protocol described previously (Hovel et al., 2012), except that 400 U of *Dpn*II and 1000 U of T4 DNA ligase were used for genomic DNA digestion and ligation, respectively. A genomic fragment devoid of the *Dpn*II sites was amplified as the control.

3C-qPCR analysis

Relative interaction frequencies were calculated by qPCR reaction (Hagege et al., 2007). In brief, the cycle threshold (Ct) values were determined for each 3C sample using combinations of the anchor primer (CF) with the rest of the VRN1 primers. We also determined the Ct value of the ADP ribosylation factor (ARF) loading control (LC) (Paolacci et al., 2009), an ARF primer set that does not span *Dpn*II restriction sites, to correct for variations in DNA concentration among the 3C samples. Thus, ratios of Ct values of the 3C product to the Ct value of ARF (LC) were calculated for all samples. Next, we corrected primer efficiencies for primer pairs using a random library (RL) as described in Weber et al. (2018). The RL was obtained by digestion of the subcloned VRN-B1 genomic region DNA with *Dpn*II restriction enzyme (NEB) and subsequent random ligation with T4 DNA ligase (NEB). We measured the Ct values of CTD for each primer pair and then used them to normalize the ratio of Ct values of all 3C samples.

Absolute quantification by qPCR

Real-time fluorescence quota PCR was used to perform the absolute quantification assay according to the protocol from Applied Biosystems. RNA was purified from wheat plumules with or without vernalization, then reverse transcribed into cDNA using the Maxima H Minus cDNA Synthesis Master Mix with dsDNase (Thermo Fisher). The cDNA samples were used as templates for PCR to amplify DNA fragments (about 200–300 bp) with primers designed based on the *TaRF2a* and *TaRF2b* sequences. The amplified fragments recovered from agarose gel were serially diluted and used as standard samples. In real-time qPCR, either cDNA samples or different concentrations of standard samples need to be added to the same reaction plate. Each reaction set contained five replicates, and the experiment was performed using the Applied Biosystems QuantStudio 3 system. Ct values of each reaction were filtered to generate and calibrate standard curves ($R^2 \geq 0.995$). The Ct values of the tested samples were required to be within the standard curve. The expressed concentration of the target genes was calculated according to the standard curve.

SUPPLEMENTAL INFORMATION

Supplemental information is available at *Molecular Plant Online*.

FUNDING

We gratefully acknowledge funding from the NSFC for the Basic Science Center Program (31788103), the National Natural Science Foundation of China (31970529), and the China Postdoctoral Science Foundation (2019M650892).

AUTHOR CONTRIBUTIONS

S.X. performed the experiments, analyzed data, and wrote the paper. Q.D., P.C., and Y.N. performed some of the experiments and data

analysis. M.D. performed the 3C-qPCR assay and analyzed the related data. J.X., L.X., Y.X., and W. Z. discussed the data analysis and polished the language of the manuscript. D.L. and C.G. designed and performed the *tarf2b* CRISPR transformation in wheat. K.C. designed the experiments, analyzed data, and polished the paper.

ACKNOWLEDGMENTS

We thank Dr. Zhuang Lu and Mrs. Jingquan Li from the Key Laboratory of Plant Molecular Physiology and the Plant Science Facility of the Institute of Botany, Chinese Academy of Sciences for their excellent technical analysis of MS/MS and technical assistance with transmission electron microscopy, respectively. We thank Professor Zhonghu He from the Institute of Crop Science, Chinese Academy of Agricultural Sciences (CAAS) for kindly providing many wheat cultivars from the core germplasm collections and for his helpful comments. We thank Professor Ben Trevaskis from CSIRO for kindly providing W15A, W11B, and W7A wheat lines, etc. No conflicts of interest declared.

Received: December 9, 2020
Revised: January 18, 2021
Accepted: May 25, 2021
Published: May 26, 2021

REFERENCES

Antoniou-Kourounioti, R.L., Hepworth, J., Heckmann, A., Duncan, S., Questa, J., Rosa, S., Sall, T., Holm, S., Dean, C., and Howard, M. (2018). Temperature sensing is distributed throughout the regulatory network that controls *FLC* epigenetic silencing in vernalization. Cell Sys. **7**:643.

Bastow, R., Mylne, J.S., Lister, C., Lippman, Z., Martienssen, R.A., and Dean, C. (2004). Vernalization requires epigenetic silencing of *FLC* by histone methylation. Nature **427**:164–167.

Chekanova, J.A. (2015). Long non-coding RNAs and their functions in plants. Curr. Opin. Plant Biol. **27**:207–216.

Chen, X.X., Ding, Y.L., Yang, Y.Q., Song, C.P., Wang, B.S., Yang, S.H., Guo, Y., and Gong, Z.Z. (2021). Protein kinases in plant responses to drought, salt, and cold stress. J. Integr. Plant Biol. **63**:53–78.

Csorba, T., Questa, J.I., Sun, Q.W., and Dean, C. (2014). Antisense COOLAIR mediates the coordinated switching of chromatin states at *FLC* during vernalization. Proc. Natl. Acad. Sci. U S A **111**:16160–16165.

Dai, S., Petruccelli, S., Ordiz, M.I., Zhang, Z., Chen, S., and Beachy, R. (2003). Functional analysis of RF2a, a rice transcription factor. J. Biol. Chem. **278**:36396–36402.

Dai, S., Wei, X., Alfonso, A., Pei, L., Duque, U., Zhang, Z., Babb, G., and Beachy, R. (2008). Transgenic rice plants that overexpress transcription factors RF2a and RF2b are tolerant to rice tungro virus replication and disease. Proc. Natl. Acad. Sci. U S A **105**:21012–21016.

Dai, S., Zhang, Z., Chen, S., and Beachy, R. (2004). RF2b, a rice bZIP transcription activator, interacts with RF2a and is involved in symptom development of rice tungro disease. Proc. Natl. Acad. Sci. U S A **101**:687–692.

Dubcovsky, J. (2005). Regulation of flowering time in wheat and barley. Comp. Biochem. Phys. A **141**:263–264.

Dubcovsky, J., Loukoianov, A., Fu, D.L., Valarik, M., Sanchez, A., and Yan, L.L. (2006). Effect of photoperiod on the regulation of wheat vernalization genes *VRN1* and *VRN2*. Plant Mol. Biol. **60**:469–480.

Fu, D.L., Szucs, P., Yan, L.L., Helguera, M., Skinner, J.S., von Zitzewitz, J., Hayes, P.M., and Dubcovsky, J. (2005). Large deletions within the first intron in *VRN-1* are associated with spring growth habit in barley and wheat. Mol. Genet. Genomics **273**:54–65.

Greenup, A., Peacock, W.J., Dennis, E.S., and Trevaskis, B. (2009). The molecular biology of seasonal flowering-responses in *Arabidopsis* and the cereals. Ann. Bot. **103**:1165–1172.

Guo, S., Xu, Y., Liu, H., Mao, Z., Zhang, C., Ma, Y., Zhang, Q., Meng, Z., and Chong, K. (2013). The interaction between OsMADS57 and OsTB1 modulates rice tillering via DWARF14. Nat. Commun. **4**:1566.

Guo, X.Y., Liu, D.F., and Chong, K. (2018). Cold signaling in plants: insights into mechanisms and regulation. J. Integr. Plant Biol. **60**:745–756.

Hagege, H., Klous, P., Braem, C., Splinter, E., Dekker, J., Cathala, G., de Laat, W., and Forne, T. (2007). Quantitative analysis of chromosome conformation capture assays (3C-qPCR). Nat. Protoc. **2**:1722–1733.

Helliwell, C.A., Robertson, M., Finnegan, E.J., Buzas, D.M., and Dennis, E.S. (2011). Vernalization-repression of *Arabidopsis FLC* requires promoter sequences but not antisense transcripts. PLoS One **6**:e21513.

Heo, J.B., and Sung, S. (2011). Vernalization-mediated epigenetic silencing by a long intronic noncoding RNA. Science **331**:76–79.

Hepworth, J., Antoniou-Kourounioti, R.L., Bloomer, R.H., Selga, C., Berggren, K., Cox, D., Harris, B.R.C., Irwin, J.A., Holm, S., Sall, T., et al. (2018). Absence of warmth permits epigenetic memory of winter in *Arabidopsis*. Nat. Commun. **9**:8.

Hovel, I., Louwers, M., and Stam, M. (2012). 3C technologies in plants. Methods **58**:204–211.

Ietswaart, R., Rosa, S., Wu, Z., Dean, C., and Howard, M. (2017). Cell-size-dependent transcription of *FLC* and its antisense long non-coding RNA COOLAIR explain cell-to-cell expression variation. Cell Sys. **4**:622.

Jung, C., and Muller, A.E. (2009). Flowering time control and applications in plant breeding. Trends Plant Sci. **14**:563–573.

Kim, D.H., and Sung, S. (2017). Vernalization-triggered intragenic chromatin loop formation by long noncoding RNAs. Dev. Cell **40**:302–312.

Kim, D.H., Xi, Y.P., and Sung, S. (2017). Modular function of long noncoding RNA, COLDAIR, in the vernalization response. PLoS Genet. **13**:e1006939.

Kippes, N., Debernardi, J.M., Vasquez-Gross, H.A., Akpinar, B.A., Budak, H., Kato, K., Chao, S., Akhunov, E., and Dubcovsky, J. (2015). Identification of the *VERNALIZATION 4* gene reveals the origin of spring growth habit in ancient wheats from South Asia. Proc. Natl. Acad. Sci. U S A **112**:E5401–E5410.

Kippes, N., Zhu, J., Chen, A., Vanzetti, L., Lukaszewski, A., Nishida, H., Kato, K., Dvorak, J., and Dubcovsky, J. (2014). Fine mapping and epistatic interactions of the vernalization gene *VRN-D4* in hexaploid wheat. Mol. Genet. Genomics **289**:47–62.

Liu, Y., Dai, S.H., and Beachy, R.N. (2007). Role of the C-terminal domains of rice (*Oryza sativa* L.) bZIP proteins RF2a and RF2b in regulating transcription. Biochem. J. **405**:243–249.

Loukoianov, A., Yan, L.L., Blechl, A., Sanchez, A., and Dubcovsky, J. (2005). Regulation of *VRN-1* vernalization genes in normal and transgenic polyploid wheat. Plant Physiol. **138**:2364–2373.

Luo, X., and He, Y. (2020). Experiencing winter for spring flowering—a molecular epigenetic perspective on vernalization. J. Integr. Plant Biol. **62**:104–117.

Marquardt, S., Raitskin, O., Wu, Z., Liu, F.Q., Sun, Q.W., and Dean, C. (2014). Functional consequences of splicing of the antisense transcript COOLAIR on *FLC* transcription. Mol. Cell **54**:156–165.

McHugh, C.A., Chen, C.K., Chow, A., Surka, C.F., Tran, C., McDonel, P., Pandya-Jones, A., Blanco, M., Burghard, C., Moradian, A.,

et al. (2015). The *Xist* lncRNA interacts directly with SHARP to silence transcription through HDAC3. Nature **521**:232–236.

Mercer, T.R., Dinger, M.E., and Mattick, J.S. (2009). Long non-coding RNAs: insights into functions. Nat. Rev. Genet. **10**:155–159.

Michaels, S.D., and Amasino, R.M. (1999). *FLOWERING LOCUS C* encodes a novel MADS domain protein that acts as a repressor of flowering. Plant Cell **11**:949–956.

Oliver, S.N., Finnegan, E.J., Dennis, E.S., Peacock, W.J., and Trevaskis, B. (2009). Vernalization-induced flowering in cereals is associated with changes in histone methylation at the *VERNALIZATION1* gene. Proc. Natl. Acad. Sci. U S A **106**:8386–8391.

Ordiz, M.I., Yang, J., Barbazuk, W.B., and Beachy, R. (2010). Functional analysis of the activation domain of RF2a, a rice transcription factor. Plant Biotechnol. J. **8**:835–844.

Ozturk, A., Caglar, O., and Bulut, S. (2006). Growth and yield response of facultative wheat to winter sowing, freezing sowing and spring sowing at different seeding rates. J. Agron. Crop Sci. **192**:10–16.

Paolacci, A.R., Tanzarella, O.A., Porceddu, E., and Ciaffi, M. (2009). Identification and validation of reference genes for quantitative RT-PCR normalization in wheat. BMC Mol. Biol. **10**:11.

Questa, J.I., Song, J., Geraldo, N., An, H.L., and Dean, C. (2016). *Arabidopsis* transcriptional repressor VAL1 triggers Polycomb silencing at *FLC* during vernalization. Science **353**:485–488.

Shi, Y.T., Ding, Y.L., and Yang, S.H. (2015). Cold signal transduction and its interplay with phytohormones during cold acclimation. Plant Cell Physiol. **56**:7–15.

Steinfort, U., Trevaskis, B., Shu, F.K., Bell, K.L., and Dreccer, M.F. (2017). Vernalisation and photoperiod sensitivity in wheat: impact on canopy development and yield components. Field Crop Res. **201**:108–121.

Song, Z.T., Liu, J.X., and Han, J.J. (2021). Chromatin remodeling factors regulate environmental stress responses in plants. J. Integr. Plant Biol. **63**:438–450.

Sun, Q.W., Csorba, T., Skourti-Stathaki, K., Proudfoot, N.J., and Dean, C. (2013). R-Loop stabilization represses antisense transcription at the *Arabidopsis FLC* locus. Science **340**:619–621.

Thorup-Kristensen, K., Cortasa, M.S., and Loges, R. (2009). Winter wheat roots grow twice as deep as spring wheat roots, is this important for N uptake and N leaching losses? Plant Soil **322**:101–114.

Tian, Y., Zheng, H., Zhang, F., Wang, S., Ji, X., Xu, C., He, Y., and Ding, Y. (2019). PRC2 recruitment and H3K27me3 deposition at *FLC* require FCA binding of COOLAIR. Sci. Adv. **5**:eaau7246.

Trevaskis, B. (2010). The central role of the *VERNALIZATION1* gene in the vernalization response of cereals. Funct. Plant Biol. **37**:479–487.

Trevaskis, B., Hemming, M.N., Dennis, E.S., and Peacock, W.J. (2007). The molecular basis of vernalization-induced flowering in cereals. Trends Plant Sci. **12**:352–357.

Weber, B., Jamge, S., and Stam, M. (2018). 3C in maize and *Arabidopsis*. Methods Mol. Biol. **1675**:247–270.

Whittaker, C., and Dean, C. (2017). The *FLC* locus: a platform for discoveries in epigenetics and adaptation. Annu. Rev. Cell Dev. Biol. **33**:555–575.

Xiao, J., Xu, S.J., Li, C.H., Xu, Y.Y., Xing, L.J., Niu, Y.D., Huan, Q., Tang, Y.M., Zhao, C.P., Wagner, D., et al. (2014). *O*-GlcNAc-mediated interaction between VER2 and TaGRP2 elicits TaVRN1 mRNA accumulation during vernalization in winter wheat. Nat. Commun. **5**:4572.

Xie, L., Zhang, Y., Wang, K., Luo, X., Xu, D., Tian, X., Li, L., Ye, X., Xia, X., Li, W., et al. (2019). TaVrt2, an SVP-like gene, cooperates with TaVrn1 to regulate vernalization-induced flowering in wheat. New Phytol. https://doi.org/10.1111/nph.16339.

Xing, L., Li, J., Xu, Y., Xu, Z., and Chong, K. (2009). Phosphorylation modification of wheat lectin VER2 is associated with vernalization-induced *O*-GlcNAc signaling and intracellular motility. PLoS One **4**:e4854.

Xu, S.J., and Chong, K. (2018). Remembering winter through vernalisation. Nat. Plants **4**:997–1009.

Xu, S.J., Xiao, J., Yin, F., Guo, X.Y., Xing, L.J., Xu, Y.Y., and Chong, K. (2019). The protein modifications of *O*-GlcNAcylation and phosphorylation mediate vernalization response for flowering in winter wheat. Plant Physiol. **180**:1436–1449.

Yan, L., Helguera, M., Kato, K., Fukuyama, S., Sherman, J., and Dubcovsky, J. (2004a). Allelic variation at the VRN-1 promoter region in polyploid wheat. Theor. Appl. Genet. **109**:1677–1686.

Yan, L.L., Loukoianov, A., Blechl, A., Tranquilli, G., Ramakrishna, W., SanMiguel, P., Bennetzen, J.L., Echenique, V., and Dubcovsky, J. (2004b). The wheat *VRN2* gene is a flowering repressor down-regulated by vernalization. Science **303**:1640–1644.

Yin, Y., Zhu, Q., Dai, S., Lamb, C., and Beachy, R. (1997). RF2a, a bZIP transcriptional activator of the phloem-specific rice tungro bacilliform virus promoter, functions in vascular development. EMBO J. **16**:5247–5259.

Yong, W.D., Xu, Y.Y., Xu, W.Z., Wang, X., Li, N., Wu, J.S., Liang, T.B., Chong, K., Xu, Z.H., Tan, K.H., et al. (2003). Vernalization-induced flowering in wheat is mediated by a lectin-like gene *VER2*. Planta **217**:261–270.

Yuan, W.Y., Luo, X., Li, Z.C., Yang, W.N., Wang, Y.Z., Liu, R., Du, J.M., and He, Y.H. (2016). A *cis* cold memory element and a *trans* epigenome reader mediate Polycomb silencing of *FLC* by vernalization in *Arabidopsis*. Nat. Genet. **48**:1527–1534.

Zhang, J.Y., Li, X.M., Lin, H.X., and Chong, K. (2019). Crop improvement through temperature resilience. Annu. Rev. Plant Biol. **70**:753–780.

Zhang, X.K., Xiao, Y.G., Zhang, Y., Xia, X.C., Dubcovsky, J., and He, Z.H. (2008). Allelic variation at the vernalization genes *Vrn-A1*, *Vrn-B1*, *Vrn-D1*, and *Vrn-B3* in Chinese wheat cultivars and their association with growth habit. Crop Sci. **48**:458–470.

Zhu, J.K. (2016). Abiotic stress signaling and responses in plants. Cell **167**:313–324.

Molecular Plant, Volume *14*

Supplemental information

The vernalization-induced long non-coding RNA *VAS* functions with the transcription factor TaRF2b to promote *TaVRN1* expression for flowering in hexaploid wheat

Shujuan Xu, Qi Dong, Min Deng, Dexing Lin, Jun Xiao, Peilei Cheng, Lijing Xing, Yuda Niu, Caixia Gao, Wenhao Zhang, Yunyuan Xu, and Kang Chong

Supplementary information

√ Supplementary Figures S1-S10

√ Supplementary Table S1-Table S2

Supplementary Figures S1-S10

Figure S1

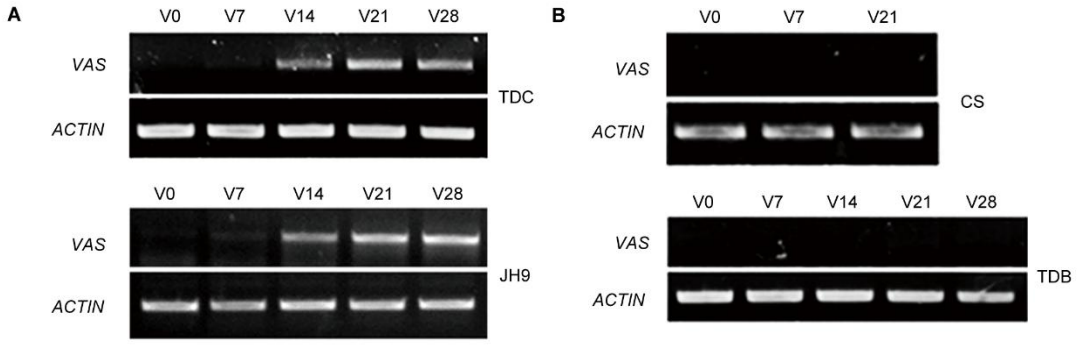

Figure S1 Expression of *VAS* in response to vernalization in different winter and spring wheats

(A) RT-PCR analysis the expression level of *VAS* in different winter wheat species, such as TDC and Jinghua9 (JH9). *ACTIN* as the loading control; (B) RT-PCR analysis the expression level of *VAS* in different spring wheat species, such as Chinese spring (CS) and TDB. *ACTIN* as the loading control.

Figure S2

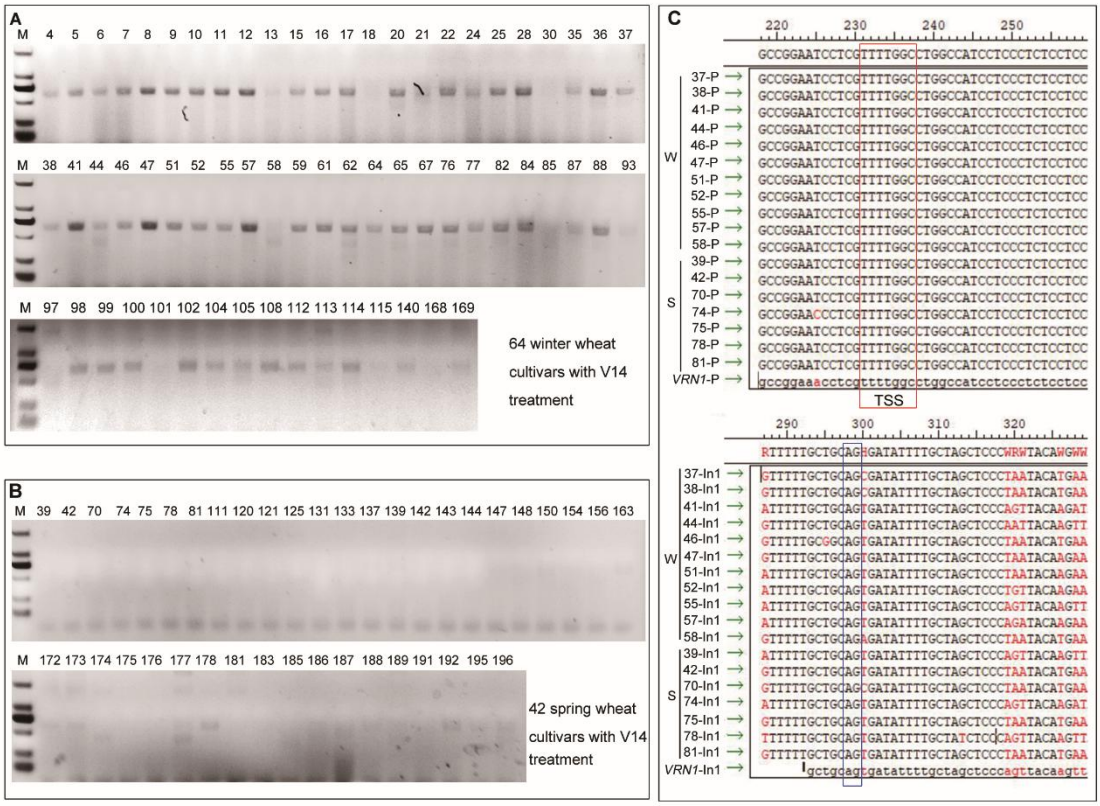

Figure S2 The detection of *VAS* in different wheats

(A) The expression of *VAS* in 64 winter wheat cultivars was detected by PCR, the vernalized-14-days samples as the template; The numbers of lanes were different cultivars (details in Supplemental table S2); (B) The expression of *VAS* in 42 spring wheat species was detected by PCR, the vernalized-14-days samples as the template; The numbers of lanes were different cultivars (details in Supplemental table S2); (C) Sequence alignments of TSS and GT-AG splice sites in winter and spring wheats.

Figure S3

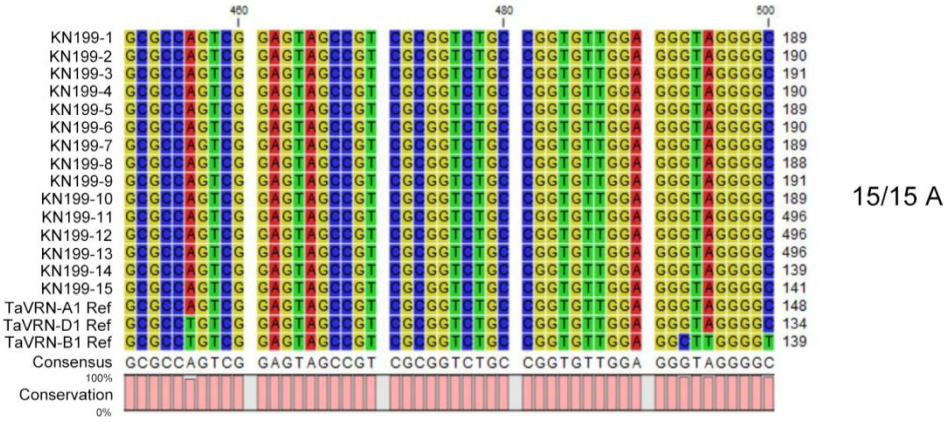

Figure S3 The alignment analysis of *VAS* sequence in KN199 wheat cultivar

TaVRN-A1 Ref, TaVRN-B1 Ref and TaVRN-D1 Ref are the promoter sequences of *TaVRN1* in different sub-genomes. 15/15 A means the 15 sequenced *VAS* transcripts are all from the A sub-genome.

Figure S4

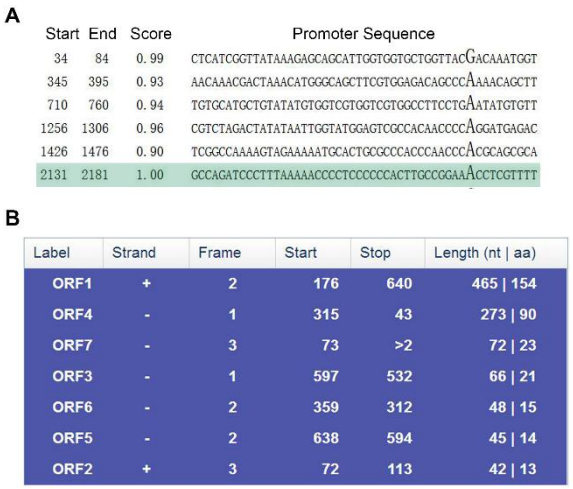

Figure S4 The sequence analysis of *VAS* transcript

(A) Prediction of transcription initiation site (TSS) of *TaVRN1* (http://www.fruitfly.org/seq_tools/promoter.html); (B) The predicted potential ORFs in the sequence of *VAS*.

Figure S5

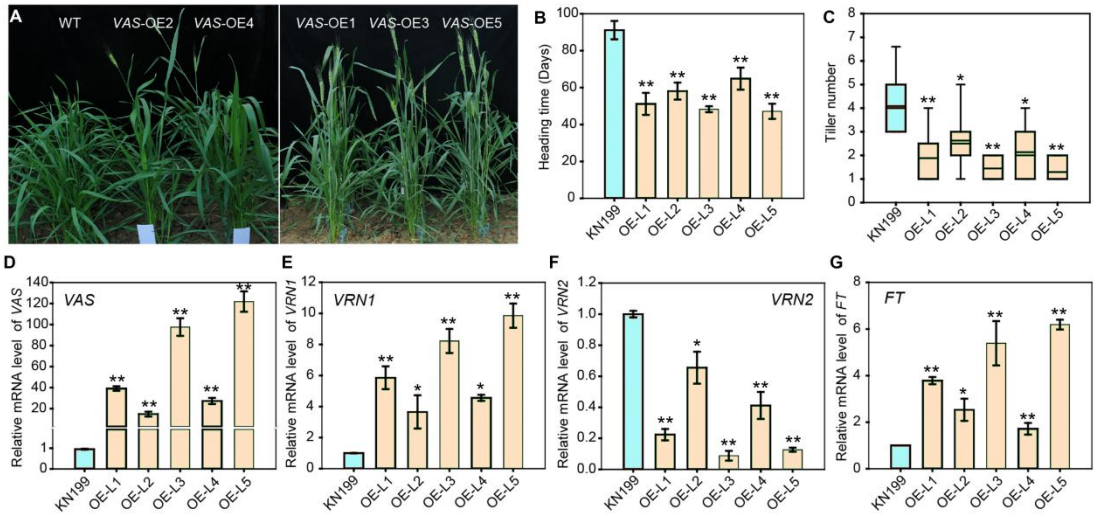

Figure S5 Overexpression of *VAS* gene promotes flowering transition in winter wheat

Morphological phenotype (A), heading time (B) and tiller number (C) (90 DAG) of *VAS*-OE transgenic wheat and wild-type KN199 (Kongnong199) with vernalized for 20 days in the greenhouse. DAG, day after germination. Data are means±s.d. of 25 plants for each line, statistical significance (two-tailed t-test) with **P < 0.01 or *P < 0.05; (D, E, F and G) Relative expression of *VAS*, *TaVRN1*, *TaVRN2* and *TaVRN3* in *VAS*-OE transgenic wheat and wild-type KN199, respectively (Data was normalized to housekeeping gene *Actin* first, then normalized to KN199 plants). Data shown are means ± SD, n=3; statistical significance (two-tailed t-test) with **P < 0.01 or *P < 0.05.

Figure S6

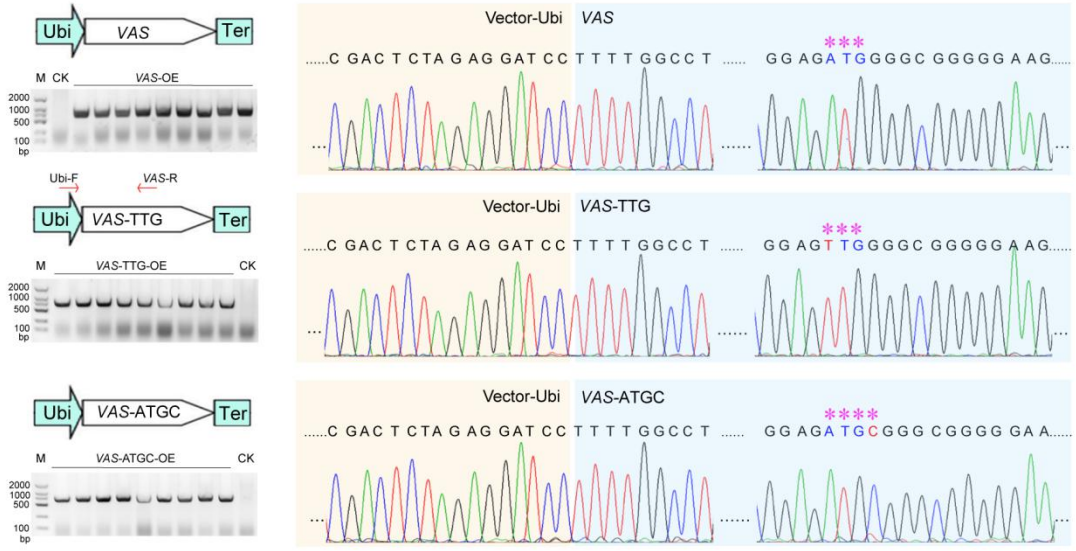

Figure S6 The PCR and sequencing identification of *VAS*-OE, *VAS*-TTG-OE and *VAS*-ATGC-OE

The primers marked with red arrows (Ubi-F and *VAS*-R). Sequences in orange background was the ubiquitin promoter of vector, and the sequences in blue background was *VAS*.

Figure S7

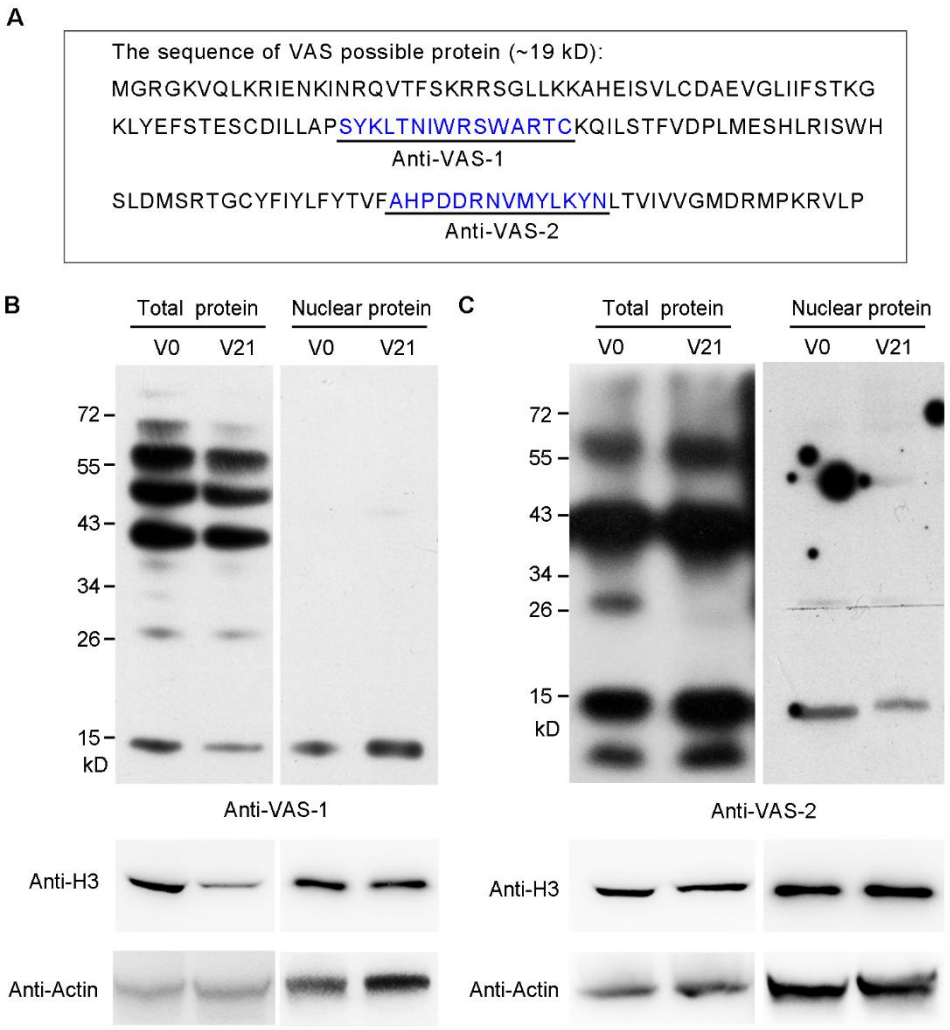

Figure S7 The detection of the VAS possible protein through Western blot

(A) The amino acid sequence of the VAS possible protein (MW about 19 kD) and the locations of the two polypeptides for preparing antibodies (Anti-VAS-1 and Anti-VAS-2); (B, C) The detection results of Western blot by using the antibodies anti-VAS-1 and anti-VAS-2, respectively, H3 antibody and Actin antibody were as loading controls; V0 means non-vernalized plumule sample, V21 means vernalied for 21 days of the plumule sample.

Figure S8

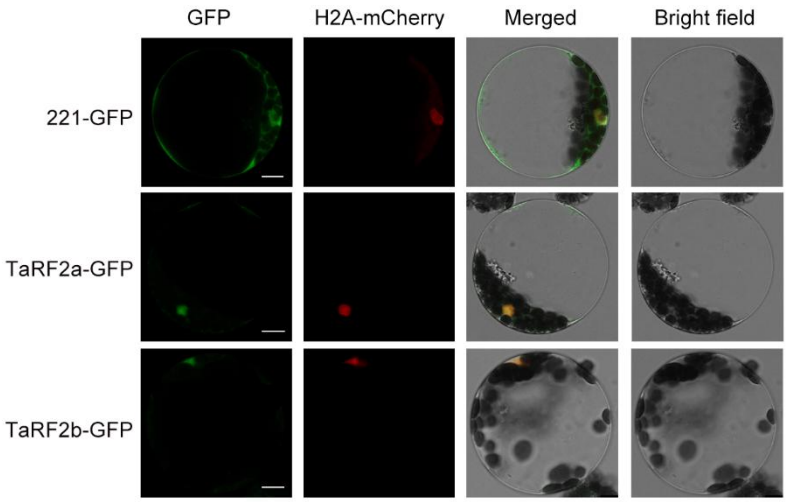

Figure S8 Nuclear localization of TaRF2a-GFP and TaRF2b-GFP

Empty GFP (pBI221-GFP) was used as negative controls. H2A-mCherry was used as the nucleus marker, Bar=10 μm.

Figure S9

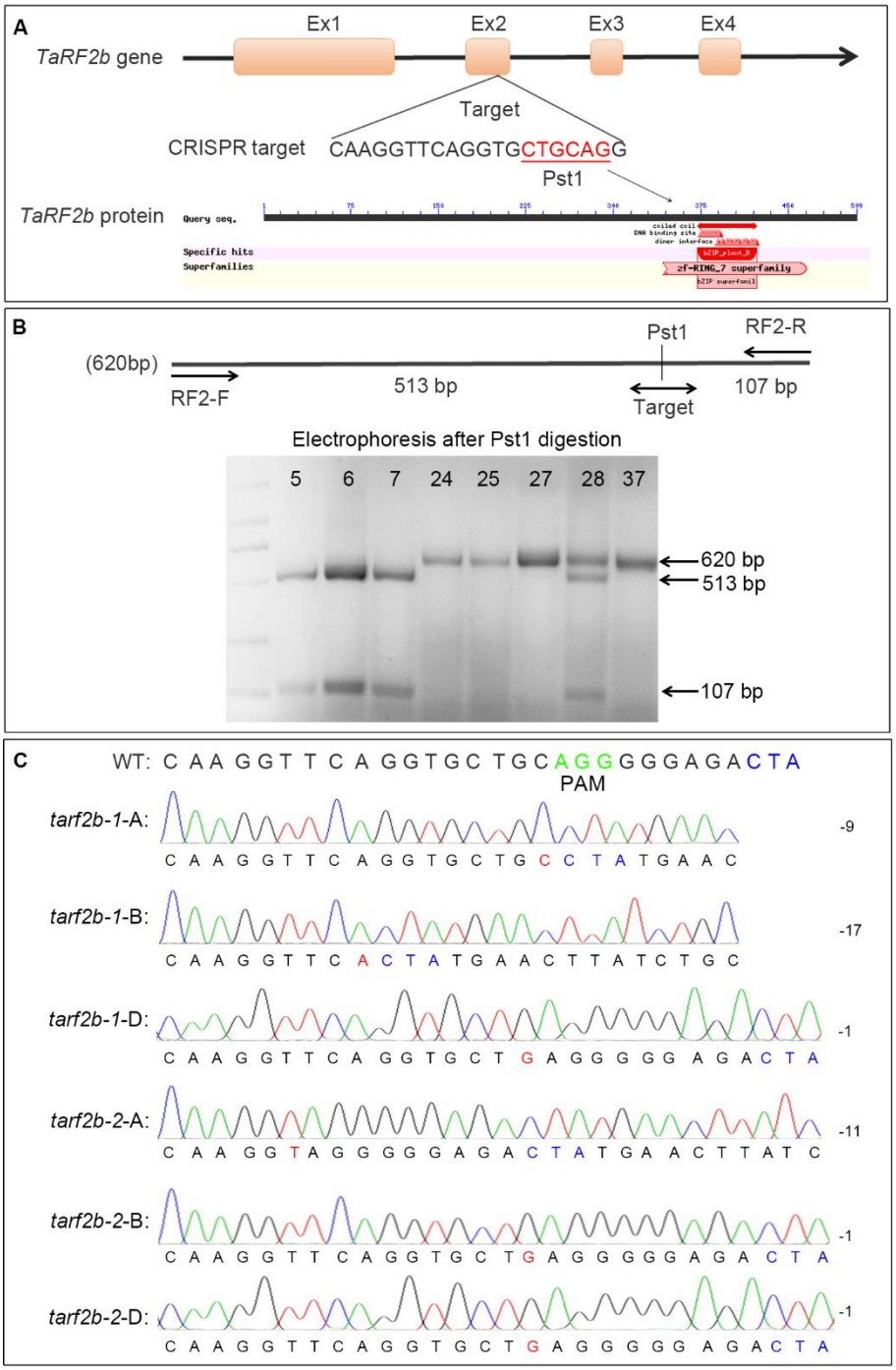

Figure S9 The identification of *tarf2b* materials

(A) The exons of *TaRF2b* and the target site of *tarf2b*-sgRNA in exon2; (B) PCR-RE assay results for 4 representative *tarf2b* mutants. Lanes 24, 25, 27 and 37 show the PCR products of the 4 mutants after PstI digestion. Lanes labelled 5, 6 and 7 are the PCR products amplified from wild type (WT) plants with PstI digestion. The sizes (bp) of the digested amplicons are

indicated on the right side; (C) Indels caused by *tarf2b*-sgRNA in the *TaRF2b-A, -B and –D* in 2 representative mutants. The PAM motif (AGG) is shown in red.

Figure S10

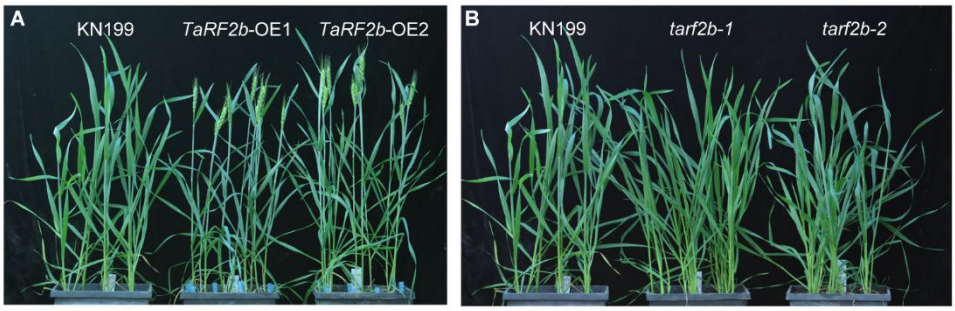

Figure S10 Morphological phenotype of *TaRF2b*-OE (A), *tarf2b* (B) transgenic wheat and wild-type KN199 with vernalization of 28 days and growth for 36 days in the greenhouse.

Supplementary Table S1

Supplementary Table S1 The list of the primers used in the manuscript.

Gene name	Primers
Real-time PCR	
VAS-Q-F	CACCAAGGGAAAGCTCTACG
VAS-Q-R	GTTAACTTGTAACTGGGAGCTAA
TaVRN1-Q-F	AAGAAGGAGAGGTCACTGCAGG
TaVRN1-Q-R	GGCTGCACTGCCGCA
TaVRN2-Q-F	CCGACACATGGCTCACCTAGTG
TaVRN2-Q-R	TTGCTTCATTGCTAATAGTGTTTGT
TaVRN3-Q-F	CAGCAGCCCAGGGTTGAG
TaVRN3-Q-R	ATCTGGGTCTACCATCACGAGTG
TaRF2a-Q-F1	TCGGAGGGAACCAGCCAATG
TaRF2a-Q-R1	TGCTGGTGCTGAGGGTGAAT
TaRF2b-Q-1007-F	CACTGTTTGCCAAAGAGTTCG
TaRF2b-Q-1106-R	TCGGTCAGCACGATCTGTG
ACTIN-Q-F	CAATCTATGAGGGATACACGCT
ACTIN-Q-R	TCAGCGGTTGTTGTGAGGGAGT
RT-PCR	
TaVAS-RT-F	CCACCAAGGGAAAGCTCTACGA
TaVAS -RT-R	TCTATCATCTGGGTGGGCGAAC
Construction of OE vectors	
TaVAS-Kpn1-F1	GGGGTACCTTTTGGCCTGGCCATCCTC
TaVAS-Sac1-R1	CGAGCTCTTAACATAAATAATTATT
TaRF2b-BamH1-F	CGGGATCCATGGATGGTGATAGCGCGCATCG
TaRF2b-Sma1-R	TCCCCCGGGGAAGTTACGCTGACGCTGTTGA
Transcription activity	
TaRF2b -DB-CZ-F	GCCATGGAGGCCGAATTC ATGGATGGTGATAGCGCGCATCG
TaRF2b -DB-CZ-R	GCTTGGCTGCAGGTCGAC GAAGTTACGCTGACGCTGTTGA
TaRF2a-DB-CZ-F	GCCATGGAGGCCGAATTC ATGAGCAGGTCTCCGGCCCCGGA
TaRF2a -DB-CZ-R	GCTTGGCTGCAGGTCGAC GTTGCCACTGCTCTCGGACCAC
5′ RACE assay	
UAP	CTACTACTACTAGGCCACGCGTCGACTAGTAC
GSP2	GGAAGTCGATAGGATCT GCTTA
Subcellular location	
TaRF2b -Xba1-F	GCTCTAGA ATGGATGGTGATAGCGCGCATCG

TaRF2b -Kpn1-R	GGGGTACC GAAGTTACGCTGACGCTGTTGA
TaRF2a -Xba1-F	GCTCTAGAATGAGCAGGTCTCCGGCCCCGGA
TaRF2a -Kpn1-R	GGGGTACCGTTGCCACTGCTCTCGGACCAC
TaRF2a and TaRF2b interaction	
TaRF2a -cluc-Kpn1-F	GGGGTACCATGAGCAGGTCTCCGGCCCCGGA
TaRF2a -cluc-BamH1-R	CGGGATCCGTTGCCACTGCTCTCGGACCAC
TaRF2b -nluc-Kpn1-F	GGGGTACCATGGATGGTGATAGCGCGCATCG
TaRF2b -nluc-Sal1-R	CGGTCGACGAAGTTACGCTGACGCTGTTGA
TaRF2a -AD-EcoR1-F	CGGAATTCATGAGCAGGTCTCCGGCCCCGGA
TaRF2a -AD-BamH1-R	CGGGATCCGTTGCCACTGCTCTCGGACCAC
TaRF2b -BD-EcoR1-F	CGGAATTC ATGGATGGTGATAGCGCGCATCG
TaRF2b -BD-BamH1-R	CGGGATCC GAAGTTACGCTGACGCTGTTGA
RF2b RIP-qPCR	
VAS-P-RIPQ-F1	GGTTCTCGAGCGGAGATG
VAS-In-RIPQ-R1	TCACATGACTCGGTGGAG
VAS-In-RIPQ-F2	ATGGAGATCCTGGGCACG
VAS-In-RIPQ-R2	TTGGCATACGGTCCATACC
VRN1-Ex1-RIPQ-F3	CAGGTGACCTTCTCCAAGC
VRN1-Ex2-RIPQ-R3	GCGCTCATACCGTTCAAG
RNA-5'Adaptor	CGACUGGAGCACGAGGACACUGACAUGGACUGAAGGA GUAGAAA
GeneRacer5'primer	GCACGAGGACACTGACATGGACTGA
GeneRacer5'nestprimer	GGACACTGACATGGACTGAAGGAGTA
GeneRacer3'primer	GCTGTCAACGATACGCTACGTAACG
GeneRacer3'nestprimer	CGCTACGTAACGGCATGACAGTG
RNA-EMSA and DNA-EMSA	
SP1-Bio-RNA	GGCUCCGCCCCCCCGCC-Bio
SP1m-Bio-RNA	GGCUCCGAAAAAAAGCC-Bio
SP1-DNA-P1	GGCTCCGCCCCCCCGCC-Bio
SP1-DNA-R1	GGCGGGGGGGCGGAGCC-Bio
SP1m-DNA-P1	GGCTCCGAAAAAAAGCC-Bio
SP1m-DNA-R1	GGCTTTTTTTCGGAGCC-Bio
Identification of OE plants and CRISPR plants	
Ubi-F	ATTATTTTGATCTTGATATACTTGGATG
VAS-R	TCCATACCAACAACAATGACTG
RF2b-R	GCTGCTGTCAACGGGGCTCCACG
RF2-F	GACAGCAGCGAGAACGAAGCCGAGAG
RF2-R	CTGGGCCAGAAAGCCTCTTGTCTGTAAG
***TaVRN1* genome identification**	
TaVRN1-79-P-F	TGTGGTGTGTGTTTGTGGCGAG
TaVRN1-1020-In1-R	AATACGCCAGATGAACAACCTT
TaVRN1-2721-In1-F	GAACCAGTTATCCTCTACACCT
TaVRN1-3436-In1-R	TTTGGTAAGATAAATGGTTGTA

Primers for TaRF2b-ChIP-qPCR	
R1-F	GTCATCTCGCCTTCCATGCCATTT
R1-R	CGCGGGACGAAACAGGAAATGC
R2-F	GGGGAAAGCAATATCGGGAGA
R2-R	GCCGCTGTCGAGCAACCATT
R3-F	TTGCTCGACAGCGGCTATGC
R3-R	GTGGTTGGGTGAGGCGGAAG
R4-F	TTCCGCCTCACCCAACCACC
R4-R	AAGCCTCCAACACCGGCAGA
UBQ-F	TATCCAACATGAATGCCACA
UBQ-R	CAGCACGAGATGAGTAAAACAA
3C related primers	
P1	GGGTACAGTAGAATAGTAGTATAAAAAGGAC
P2	GGCATCGTGTGGCTGCAGTA
P3	CATCCTCCCTCTCCTCCCTCT
I1	GCCTCATCATCTTCTCCACCAAGG
I2	GGACCTGGTTTGGATAATGGTTAATGTACCC
I3	GCCCTCAGGATTTCATGGCATAGTCT
I4	GGTAATTTTGTTTCTTTGTGCCCCCC
I5	GCGGTAGGCGCTAATCGTGAA
3C-qPCR related primers	
3C-CF	GTCTGCCGGTGTTGGAGGCT
3C-VRN1B-Taqman	TTGGCCCCGTTCTCCAGCGGAGA
3C-VRN1-F1	TCGCCCTCAGGATTTCATGG
3C-VRN1-F2	TCCGCATAGTGCATCAAACC
3C-VRN1-F3	GTGGGCTGCGAGTCAAGGTT
3C-ARF-Taqman	CCACATCCCAAACAGTGAAGCTGA
3C-ARF-F	TGCAGGATTTAACGTCGAAAC
3C-ARF-R	AAGGAACAGATTCACAAAGGG
VAS sequence analysis	
VAS-1-F	TTTTGGCCTGGCCATCCTCCCTCTC
VAS-610-R	TACCAACAACAATGACTGTGAG
M13F	TGTAAAACGACGGCCAGT

Supplementary Table S2

Supplementary table S2 The list of the wheat cultivars used in figure S2

Number	wheat cultivars	Growth habit	Number	wheat cultivars	Growth habit
4	Zhongmai 9	W	88	Zhoumai 18	W
5	Zhongyou 9507	W	93	Bima 4	W
6	Lunxuan 987	W	97	Aifeng 3	W
7	CA9722	W	98	Shannong 7859	W
8	CA0045	W	99	Shan 229	W
9	CA8686	W	100	Shanyou 225	W
10	CA9632	W	101	Xiaoyan 6	W
11	Jing 411	W	102	Xiaoyan 22	W
12	Jing 9428	W	104	Jinmai 33	W
13	Fengkang 2	W	105	Jinmai 45	W
15	Jingdong 6	W	108	Xuzhou 25	W
16	Jingdong 8	W	111	Huaimai 18	S
17	Jingdong 10	W	112	Huaimai 20	W
18	Nongda 139	W	113	Wanmai 18	W
20	Nongda 3214	W	114	Wanmai 19	W
21	Nongda 3291	W	115	Wanmai 38	W
22	Dongfanghong 3	W	120	Yangmai 2	S
24	Jingwang 10	W	121	Yangmai 3	S
25	Jingshuang 6	W	125	Yang mai 10	S
28	Jinmai 60	W	131	Sumai 3	S
30	Xifeng 1	W	133	Ningmai 9	S
35	Jimai 36	W	137	Shen 32109	S
36	Jimai 38	W	139	Een 1	S
37	Shijiazhuang 8	W	140	Emai 6	W
38	Shijiazhuang 407	W	142	Emai 12	S
39	Shi 4185	S	143	Emai 14	S
41	Han 6172	W	144	Huamai 8	S
42	Heng 7228	S	147	Wanmai 48	S
44	Taishan 1	W	148	Chenduguangtou	S
46	Jinan 2	W	150	Fan 6	S
47	Jinan 9	W	154	Chuanmai 24	S
51	Jimai 19	W	156	Chuanmai 107	S
52	Jimai 20	W	163	Mianyang 26	S
55	Lumai 14	W	168	Zhongnong 28	W
57	Lumai 21	W	169	Ailiduo	W
58	Lumai 22	W	172	Yunmai 42	S
59	Lumai 23	W	173	Yunmai 46	S

61	Yannong 15	W	174	Fengmai 24	S
62	Yanyou 361	W	175	Fengmai 27	S
64	Zimai 12	W	176	Fengmai 29	S
65	Weimai 8	W	177	Yumai 3	S
67	Wendengbianmai	W	178	Demai 3	S
70	Pingyuan 50	S	181	Jingmai 11	S
74	Neixiang 36	S	183	Kehan 6	S
75	Zhengmai 9023	S	185	Kefeng 6	S
76	Xin 9408	W	186	Xinkehan 9	S
77	Yumai 2	W	187	Longfumai 1	S
78	Yumai 7	S	188	Longfumai 2	S
81	Yumai 18	S	189	Longfumai 3	S
82	Yumai 21	W	191	Longfumai 5	S
84	Yumai 49	W	192	Longfumai 8	S
85	Yumai 54	W	195	Longfumai 12	S
87	Yumai 70	W	196	Longfumai13	S

**The detail information is included in the reference (Zhang et al., 2008).